Highlights

Sampling-based sensitivity indices for stochastic solvers with application to Monte Carlo radiation transport

Kayla B. Clements, Gianluca Geraci, Aaron J. Olson, Todd S. Palmer

- An approach is developed for global sensitivity analysis using stochastic computational solvers.
- Variance deconvolution, in which solver variance is explicitly calculated and removed from the total observed variance, is briefly reviewed.
- Variance deconvolution is combined with existing methods for Sobol' indices.
- Statistical properties of the variance deconvolution estimator are compared with those of the standard approach both analytically and with numerical exploration.
- For the Ishigami problem, indices using variance deconvolution converge to the known solution for a lower computational cost than the standard approach.
- Monte Carlo radiation transport is used for an additional numerical example.

Sampling-based sensitivity indices for stochastic solvers with application to Monte Carlo radiation transport

Kayla B. Clements[a,*], Gianluca Geraci[b,*], Aaron J. Olson[b], Todd S. Palmer[a]

[a] *Oregon State University, Address, Corvallis, OR, USA*
[b] *Sandia National Laboratories, P.O. Box 5800, Mail Stop 1318, Albuquerque, 87185-1318, NM, USA*

Abstract

In computational modeling, global sensitivity analysis aims to characterize how input variability affects output variability. Sobol' indices, a variance-based tool for global sensitivity analysis, rank parameters in order of importance to model response across the entire combined input parameter space. Accurate and efficient methods for computing Sobol' indices have been widely researched for deterministic simulators, in which multiple evaluations of the same input will produce identical outputs. Stochastic simulators, on the hand, have an intrinsic randomness and produce different outputs for multiple evaluations of the same input. This introduces additional variability to model output, complicating the use of traditional methods for computing Sobol' indices. In this paper, we focus on computing Sobol' indices that are unbiased by solver noise without needing to over-resolve each evaluation of the stochastic simulator. We propose doing so using variance deconvolution, in which we explicitly calculate the variance due to the solver and remove it from the total observed variance. The proposed method is applied to two examples – the Ishigami function that is commonly used as a test case for Sobol' indices and a neutron-transport case study. The results confirm the convergence of the approach and highlight the approach's utility particularly when the indices are not near-zero and when there is a large amount of solver noise.

Keywords: global sensitivity analysis, Monte Carlo radiation transport, stochastic solvers, sobol indices

1. Introduction

In computational modeling, uncertainty and sensitivity analyses are essential to quantify and analyze the reliability, accuracy, and robustness of a model and its outputs [1, 2, 3]. Uncertainty analysis focuses on quantifying uncertainty in model output by calculating statistics of the quantity of interest such as mean and variance [4, 5]; it is also referred to as uncertainty quantification (UQ). Sensitivity analysis (SA), a related practice, is the study of how uncertainty in model output can be ascribed to different sources of input uncertainty [6]. *Local* SA characterizes a system's response to small perturbations around some nominal parameter value by computing partial derivatives of the model response at that value [7, 8]. On the other hand, *global* sensitivity analysis (GSA) aims to rank parameters in order of importance to model response across the entire input parameter space. There are many statistics that can be used as measures of importance for parameter ranking; what statistic is used depends on what question the practitioner hopes to answer, defined in [4] as the SA *setting*. For an exhaustive introduction to GSA in the scientific computing context, see Saltelli's book [4].

In this paper we focus on variance-based GSA, in which sensitivity indices are used to determine which factor or set of factors has the largest impact on output variance. Sensitivity indices (SIs), also commonly referred to as Sobol' indices, arise from the ANOVA (ANalysis Of VAriance) decomposition of the output [9, 10]. Many methods have been introduced to compute SIs, either by approximating the ANOVA decomposition via meta-modeling (surrogate modeling) or directly by using a sampling-based approach. In the former, the ANOVA decomposition

*Corresponding authors

Email addresses: clemekay@oregonstate.edu,kbcleme@sandia.gov (Kayla B. Clements), ggeraci@sandia.gov (Gianluca Geraci), aolson@sandia.gov (Aaron J. Olson), todd.palmer@oregonstate.edu (Todd S. Palmer)

of the output is approximated via a surrogate model, such as the polynomial chaos expansion [11]. Meta-modeling approaches typically require fewer model evaluations than sampling-based approaches and are therefore attractive for computational models with a large single-simulation time; however, they can be susceptible to any lack of smoothness or regularity of the underlying function [4, 11] and suffer from the 'curse of dimensionality' [12, 11]. In the latter, indices are computed directly using sampling-based estimators in combination with sampling schemes such as Monte Carlo (MC), quasi-MC, or Latin Hypercube [9, 10, 13]. Sampling-based methods are useful because they do not make any *a priori* assumptions about the linearity, smoothness, or regularity of the model [14, 8]. They do assume that the input factors are mutually independent [15], though treatments exist for the more complex case of correlated input factors [4]. Their primary drawback is the high computational cost associated with the multiple code evaluations needed to compute a full suite of sensitivity indices, and efficient numerical algorithms for computing SIs is an area of ongoing research [16].

The vast majority of the large body of work on GSA [4, 3, 7, 8] has been designed with deterministic solvers in mind, inherently assuming that output variability results exclusively from propagated input variability. Additional complication arises when performing sensitivity analysis in the context of stochastic solvers, which are used in a variety of disciplines such as compute networks [17, 18], turbulent flows [19], financial modeling [20], disease prediction [21], and radiation transport [22]. Multiple evaluations of a stochastic solver using the same input will produce different outputs, akin to different realizations of a random variable whose probability distribution is unknown [23]. In computer codes, stochastic solvers simulate randomness using (pseudo-)random number generators, where the initial seed could be chosen by the analyst but the random number stream cannot [24]. When the inputs of a stochastic simulator have some associated uncertainty, as is the case for GSA, the total observed output variance is a combination of the variability of the solver itself (referred to from here as solver variance) and the variability of the inputs (referred to from here as parametric variance) [25, 26]. A standard approach to approximate the parametric variance using a stochastic solver is to increase the number of solver realizations, knowing that the total variance will approach the parametric variance in the limit of an infinite number of solver samples [27]. However, doing this for each of the multiple code evaluations needed to calculate sampling-based SIs exacerbates the already-high computational cost.

Over the past decade or so, there have been a number of methods introduced to extend Sobol' indices to stochastic simulators, which are reviewed thoroughly in [28]. The macroparameter method [29] considers the solver's random seed to be an additional input parameter and computes Sobol' indices as if there are $(k + 1)$ parameters, explicitly treating the covariances [30] of the sets of k now-correlated inputs (similar methods exist for sampling-based UQ with stochastic solvers, e.g., Total Monte Carlo [31, 32]). Other methods have defined the Sobol' indices themselves as random variables by treating them as functions of the solver stochasticity, then analyzed the statistical properties of the SIs [33, 34]. Many of the proposed methods mitigate the expense of resolving the stochastic solver by instead emulating the stochastic solver with a surrogate model, then calculating Sobol' indices using the constructed surrogate at a reduced computational cost [28]. One such class of methods uses joint meta-models to deterministically represent the statistics of the stochastic outputs such as mean and variance [29, 35], alpha-quantile [36], and differential entropy [37]. Most recently, Zhu and Sudret [28] presented a framework for creating a surrogate that captures entire response distribution of the stochastic solver by using their generalized lambda model.

In recent publications [38], as an alternative to the standard approach, we proposed a novel method for UQ with stochastic solvers called *variance deconvolution* to compute parametric variance without a surrogate by explicitly quantifying and removing the solver variance from the total observed variance. In Clements, *et al.* [26], we rigorously showed that variance deconvolution is accurate and far more cost effective than the standard approach for computing parametric variance. In previous work, we integrated variance deconvolution in sampling-based GSA for stochastic media [38] and surrogate [39, 40] approaches. The goal of this paper is to present a clear framework to compute Sobol' indices using stochastic solvers without stochastic emulators or the expensive standard approach by using variance deconvolution. We examine the biases introduced when using stochastic solvers to compute parametric SIs, discuss how and when to use variance deconvolution, and analyze the impact of combining it with existing sampling-based methods for SIs.

The remainder of the paper is structured as follows. In Section 2, we review ANOVA decomposition and Sobol' indices. In Section 3, we review existing sampling-based estimators for sensitivity indices. In Section 4, we summarize variance deconvolution as presented in [26]. Then, in Section 5, we discuss the impact of computing SIs with stochastic solvers and how using variance deconvolution compares to a standard approach. In Section 6, we show variance deconvolution's performance and compare it to that of the standard approach for two examples, the analytical Ishigami function and a neutral-particle radiation transport example problem with energy-dependence and fission. Finally, we summarize the main findings of the paper and discuss possible future applications in Section 7.

2. Background and theory on ANOVA

In this section, we give a brief review of Sobol's variance decomposition [9] and how it is used to define variance-based sensitivity indices [9, 10].

2.1. Sobol' decomposition

Consider a generic scalar quantity of interest (QoI) $Q = Q(\boldsymbol{\xi}), \boldsymbol{\xi} = (\xi_1, \ldots, \xi_k) \in \Xi \subset \mathbb{R}^k$, where $\xi_1, \ldots, \xi_k$ are independent random variables with arbitrary joint distribution function $p(\boldsymbol{\xi})$. The mean and variance of Q can be computed as

$$\mathbb{E}_\xi [Q] = \int_\Xi Q(\boldsymbol{\xi})\, p(\boldsymbol{\xi}) d\boldsymbol{\xi} \qquad \text{and} \qquad \mathbb{V}ar_\xi [Q] = \int_\Xi \left(Q(\boldsymbol{\xi}) - \mathbb{E}_\xi [Q] \right)^2 p(\boldsymbol{\xi}) d\boldsymbol{\xi}, \tag{1}$$

respectively, where we have used a subscript to indicate the expectation and variance over ξ. Sobol' considered [9] an expansion of Q into 2^k orthogonal terms of increasing dimension,

$$Q = Q_0 + \sum_i Q_i + \sum_i \sum_{j>i} Q_{ij} + \cdots + Q_{12\ldots k}, \tag{2}$$

in which each term is a function only of the factors in its subscript, i.e., $Q_i = Q_i(\xi_i)$, $Q_{ij} = Q_{ij}(\xi_i, \xi_j)$. In particular, Sobol' considered the case in which each term could be defined recursively using the conditional expectations of Q,

$$Q_0 = \mathbb{E}_\xi [Q] \tag{3}$$

$$Q_i = \mathbb{E}_{\xi_{\sim i}} \left[Q \mid \xi_i \right] - Q_0 \tag{4}$$

$$Q_{ij} = \mathbb{E}_{\xi_{\sim i}, \xi_{\sim j}} \left[Q \mid \xi_i, \xi_j \right] - Q_i - Q_j - Q_0, \tag{5}$$

where $\mathbb{E}_{\xi_{\sim i}} \left[Q \mid \xi_i \right]$ indicates the expected value of Q conditional on some fixed value ξ_i and $\mathbb{E}_{\xi_{\sim i}, \xi_{\sim j}} \left[Q \mid \xi_i, \xi_j \right]$ indicates the expected value of Q conditional on the pair of values (ξ_i, ξ_j). The variances of the terms in Eq. (2) give rise to the measures of importance being sought. The conditional variance $\mathbb{V}ar_\xi [Q_i] = \mathbb{V}ar_{\xi_i} \left[\mathbb{E}_{\xi_{\sim i}} \left[Q \mid \xi_i \right] \right] \stackrel{\text{def}}{=} \mathbb{V}_i$ is called the first-order effect of ξ_i on Q. The second-order effect $\mathbb{V}ar_\xi \left[Q_{ij} \right] = \mathbb{V}ar \left[\mathbb{E} \left(Q \mid \xi_i, \xi_j \right) \right] - \mathbb{V}_i - \mathbb{V}_j \stackrel{\text{def}}{=} \mathbb{V}_{ij}$ is the difference between the combined effect of the pair (ξ_i, ξ_j) and both of their individual effects; it captures the effect solely of their interaction with one another. Higher-order effects can be defined analogously to quantify the effects of higher-order interactions, up to the final term $\mathbb{V}_{12\ldots k}$. Sobol's variance decomposition expands $\mathbb{V}ar_\xi [Q]$ into variance terms of increasing order,

$$\mathbb{V}ar_\xi [Q] = \sum_i \mathbb{V}_i + \sum_i \sum_{j>i} \mathbb{V}_{ij} + \cdots + \mathbb{V}_{12\ldots k}. \tag{6}$$

Sensitivity indices (SIs), also referred to as Sobol' indices, result directly from dividing Eq. (6) by the unconditional variance $\mathbb{V}ar [Q]$ and provide measures of importance used to, e.g., rank the parameters in GSA; this is discussed in the next section.

2.2. Sensitivity indices

A sensitivity index is the ratio of the conditional variance of a parameter or set of parameters to the unconditional variance, which can be used as a measure of importance of the parameter(s) to the QoI [9, 10, 41, 42, 43]. The first-order sensitivity index of parameter ξ_i on Q is the ratio of its first-order effect to the unconditional variance,

$$\mathbb{S}_i = \frac{\mathbb{V}ar_{\xi_i}\left[\mathbb{E}_{\xi_{\sim i}}\left[Q \mid \xi_i\right]\right]}{\mathbb{V}ar_{\xi}\left[Q\right]}. \tag{7}$$

The k first-order SIs represent the main effect contributions of each input factor to the variance of the output. All first-order SIs are between 0 and 1. Analogously to the higher-order variance terms in Eq. (6), higher-order SIs represent the contribution only of the interactions amongst a set of variables. Dividing Eq. (6) by $\mathbb{V}ar_{\xi}\left[Q\right]$ results in the summation of all of the first- and higher-order SIs to 1:

$$1 = \sum_i \mathbb{S}_i + \sum_i \sum_{j>i} \mathbb{S}_{ij} + \cdots + \mathbb{S}_{12\ldots k}, \tag{8}$$

such that, by definition, $\sum_{i=1}^{k} \mathbb{S}_i \leq 1$. A parameter's contribution can also be described by its total-order SI $\mathbb{T}_i$, which accounts for its total contribution to the output variance by summing its first-order effect and all of its higher-order effects. For example, in a model with three parameters, the total effect of ξ_1 would be the sum of all of the terms in Eq. (8) that contain a 1: $\mathbb{T}_1 = \mathbb{S}_1 + \mathbb{S}_{12} + \mathbb{S}_{13} + \mathbb{S}_{123}$.

The total-order SI of ξ_i can be expressed [10, 15] by conditioning on the set $\boldsymbol{\xi}_{\sim i}$, which contains all factors except ξ_i, as

$$\mathbb{T}_i = 1 - \frac{\mathbb{V}ar_{\xi_{\sim i}}\left[\mathbb{E}_{\xi_i}\left[Q \mid \boldsymbol{\xi}_{\sim i}\right]\right]}{\mathbb{V}ar_{\xi}\left[Q\right]} = \frac{\mathbb{E}_{\xi_{\sim i}}\left[\mathbb{V}ar_{\xi_i}\left[Q \mid \boldsymbol{\xi}_{\sim i}\right]\right]}{\mathbb{V}ar_{\xi}\left[Q\right]}. \tag{9}$$

The conditional variance $\mathbb{V}ar_{\xi_i}\left[\mathbb{E}_{\xi_{\sim i}}\left[Q \mid \boldsymbol{\xi}_{\sim i}\right]\right]$ can be understood as the main effect of everything that is not ξ_i; when it is subtracted from $\mathbb{V}ar_{\xi}\left[Q\right]$, the remaining $\mathbb{E}_{\xi_{\sim i}}\left[\mathbb{V}ar_{\xi_i}\left[Q \mid \boldsymbol{\xi}_{\sim i}\right]\right] \stackrel{\text{def}}{=} \mathbb{E}_{\sim i}$ is the effect of all terms that *do* contain ξ_i.

Rather than compute every term in Eq. (8) to fully characterize the effect of parameter ξ_i, it is customary to compute the set of first- and total-order indices for a good description of the importance of parameters and their interactions at a reasonable cost [4]. In the next section, we summarize sampling-based methods for estimating the full set of first- and total-order SIs.

3. Sampling-based estimators for sensitivity indices

The development of efficient numerical algorithms for computing the full suite of first- and total-order SIs has been an ongoing area of research since MC estimators for $\mathbb{S}_i$ and $\mathbb{T}_i$ were first proposed [9, 10, 15], and a number of sampling schemes and estimators exist to do so. The various methods follow the same general structure: sample the parameter space, evaluate the computational model at the sampled parameters, then approximate $\mathbb{S}_i$ and $\mathbb{T}_i$ using MC estimators. We outline the general algorithm, the Saltelli approach [44, 15], here, assuming k uncertain parameters:

1. Define two (N_{ξ}, k) matrices, $\boldsymbol{A}$ and $\boldsymbol{B}$, which contain independent input samples.

$$\boldsymbol{A} = \begin{bmatrix} \xi_1^{(1)} & \cdots & \xi_i^{(1)} & \cdots & \xi_k^{(1)} \\ \vdots & & \ddots & & \vdots \\ \xi_1^{(N)} & \cdots & \xi_i^{(N_{\xi})} & \cdots & \xi_k^{(N_{\xi})} \end{bmatrix}, \quad \boldsymbol{B} = \begin{bmatrix} \xi_{k+1}^{(1)} & \cdots & \xi_{k+i}^{(1)} & \cdots & \xi_{2k}^{(1)} \\ \vdots & & \ddots & & \vdots \\ \xi_{k+1}^{(N_{\xi})} & \cdots & \xi_{k+i}^{(N_{\xi})} & \cdots & \xi_{2k}^{(N_{\xi})} \end{bmatrix}. \tag{10}$$

2. For each i-th parameter, define matrix $\boldsymbol{A}_{\boldsymbol{B}}^{(i)}$ ($\boldsymbol{B}_{\boldsymbol{A}}^{(i)}$), which is a copy of $\boldsymbol{A}$ ($\boldsymbol{B}$) except for the i-th column, which comes from $\boldsymbol{B}$ ($\boldsymbol{A}$).

$$\boldsymbol{A}_{\boldsymbol{B}}^{(i)} = \begin{bmatrix} \xi_1^{(1)} & \cdots & \xi_{k+i}^{(1)} & \cdots & \xi_k^{(1)} \\ \vdots & & \ddots & & \vdots \\ \xi_1^{(N_{\xi})} & \cdots & \xi_{k+i}^{(N_{\xi})} & \cdots & \xi_k^{(N_{\xi})} \end{bmatrix}. \tag{11}$$

3. Compute model output for $\boldsymbol{A}$, $\boldsymbol{B}$, and all $\boldsymbol{A}_{\boldsymbol{B}}^{(i)}$ ($\boldsymbol{B}_{\boldsymbol{A}}^{(i)}$) to obtain vectors of model output $Q(\boldsymbol{A})$, $Q(\boldsymbol{B})$, $Q(\boldsymbol{A}_{\boldsymbol{B}}^{(i)})$, and/or $Q(\boldsymbol{B}_{\boldsymbol{A}}^{(i)})$ of dimension $(N_\xi, 1)$.
4. Approximate the full set of $\mathbb{S}_i$ and $\mathbb{T}_i$ using $Q(\boldsymbol{A})$, $Q(\boldsymbol{B})$, $Q(\boldsymbol{A}_{\boldsymbol{B}}^{(i)})$, and/or $Q(\boldsymbol{B}_{\boldsymbol{A}}^{(i)})$.

Specific methods for computing SIs are defined by two components [45]: 1) the sampling scheme used to populate matrices $\boldsymbol{A}$ and $\boldsymbol{B}$ from the parameter space, such as purely random MC or a quasi-random scheme like the Sobol' sequence [46, 47] or Latin hypercube [48]; and 2) the MC estimators used to approximate Eqs. (7) and (9). Though some estimators require a specific sampling scheme, quasi-random sampling as a default choice has been shown to be the best for a function of unknown behavior [13, 49]. This is by no means intended as an exhaustive review of estimator design; a few notable works include [4, 9, 10, 15, 44, 50, 51, 52, 53, 54, 55, 56, 57, 58, 59, 60, 61, 62, 63, 64]. For a review, see, e.g., [44, 16].

For simplicity when examining the effects of variance deconvolution, we limit discussion to using purely random MC sampling. With purely random MC sampling, there is no difference between using triplet $\left(\boldsymbol{A}, \boldsymbol{B}, \boldsymbol{A}_{\boldsymbol{B}}^{(i)}\right)$ or triplet $\left(\boldsymbol{B}, \boldsymbol{A}, \boldsymbol{B}_{\boldsymbol{A}}^{(i)}\right)$ in the estimators, as long as they are used consistently within the estimator [44]. We also limit discussion to one first- and one total-order estimator, shown in Section 3.1. Later, we discuss how the presented variance deconvolution analysis can be extended to other SI estimators.

3.1. Sampling estimators for $\mathbb{S}_i$ and $\mathbb{T}_i$

As recommended by Saltelli et al. (2012) [65], we use the the sampling estimator for $\mathbb{S}_i$ from Sobol' et al. (2007) [58] and for $\mathbb{T}_i$ from Jansen et al. (1999) [59]. Letting $Q(\boldsymbol{A})_v$ indicate the v-th element of the vector $Q(\boldsymbol{A})$, i.e., one function evaluation of Q,

$$\mathbb{S}_i \approx \frac{\frac{1}{N_\xi}\sum_{v=1}^{N_\xi} Q(\boldsymbol{B})_v \left[Q(\boldsymbol{A}_{\boldsymbol{B}}^{(i)})_v - Q(\boldsymbol{A})_v\right]}{\frac{1}{2N_\xi}\sum_{v=1}^{N_\xi}\left[Q(\boldsymbol{A})_v - Q(\boldsymbol{B})_v\right]^2} \stackrel{\text{def}}{=} \hat{\mathbb{S}}_i, \tag{12}$$

$$\mathbb{T}_i \approx \frac{\frac{1}{2N_\xi}\sum_{v=1}^{N_\xi}\left[Q(\boldsymbol{A}_{\boldsymbol{B}}^{(i)})_v - Q(\boldsymbol{A})_v\right]^2}{\frac{1}{2N_\xi}\sum_{v=1}^{N_\xi}\left[Q(\boldsymbol{A})_v - Q(\boldsymbol{B})_v\right]^2} \stackrel{\text{def}}{=} \hat{\mathbb{T}}_i. \tag{13}$$

In the following, we analyze how to compute the statistical quantities introduced above when the underlying QoI is computed using a stochastic solver.

4. Introduction to variance deconvolution

Variance deconvolution was introduced [26, 38] as a means to efficiently and accurately estimate the parametric variance of QoI Q in the presence of an additional variance contribution from a stochastic solver. In this section, we summarize the concept and notation of variance deconvolution before extending it to GSA in Section 5. For a detailed presentation of variance deconvolution, see [26].

We consider the same generic QoI defined in Section 1, $Q = Q(\boldsymbol{\xi}), \boldsymbol{\xi} = (\xi_1, \ldots, \xi_k) \in \Xi \subset \mathbb{R}^k$, with mean $\mathbb{E}_\xi[Q]$ and variance $\mathbb{V}ar_\xi[Q]$. We additionally introduce a random variable η to represent the inherent variability of the stochastic solver, and define our QoI Q as the expectation over η of a function $f(\boldsymbol{\xi}, \eta)$, $Q(\boldsymbol{\xi}) \stackrel{\text{def}}{=} \mathbb{E}_\eta[f(\boldsymbol{\xi}, \eta)]$. The function $f(\boldsymbol{\xi}, \eta)$ can be directly evaluated as the output from the stochastic solver with input $\boldsymbol{\xi}$, but the expectation $\mathbb{E}_\eta[f(\boldsymbol{\xi}, \eta)]$ and variance $\sigma_\eta^2(\boldsymbol{\xi}) \stackrel{\text{def}}{=} \mathbb{V}ar_\eta[f(\boldsymbol{\xi}, \eta)]$ are not directly available. Instead, we approximate $Q(\boldsymbol{\xi})$ and $\sigma_\eta^2(\xi)$ as the sample mean and variance of f over N_η independent evaluations:

$$Q(\boldsymbol{\xi}) \approx \frac{1}{N_\eta}\sum_{j=1}^{N_\eta} f(\boldsymbol{\xi}, \eta^{(j)}) \stackrel{\text{def}}{=} \tilde{Q}_{N_\eta}(\boldsymbol{\xi}) \quad \text{and} \quad \sigma_\eta^2(\boldsymbol{\xi}) \approx \frac{1}{N_\eta - 1}\sum_{j=1}^{N_\eta}\left(f(\boldsymbol{\xi}, \eta^{(j)}) - \tilde{Q}_{N_\eta}(\boldsymbol{\xi})\right)^2 \stackrel{\text{def}}{=} \hat{\sigma}_\eta^2(\boldsymbol{\xi}).$$

In the context of MC RT, $\eta^{(j)}$ corresponds to the internal stream of random numbers comprising a single particle history, $f(\boldsymbol{\xi}, \eta^{(j)})$ corresponds to the result (e.g., tally) of that single particle history, and $\tilde{Q}_{N_\eta}(\boldsymbol{\xi})$ corresponds to the output of a MC RT simulation that used a total of N_η particle histories. In [26], we present that the total variance of $\tilde{Q}_{N_\eta}$ decomposes into the effect of the uncertain parameters and the effect of the stochastic solver,

$$\mathbb{V}ar_{\xi}\left[Q\right] = \mathbb{V}ar\left[\tilde{Q}_{N_\eta}\right] - \frac{1}{N_\eta}\mathbb{E}_{\xi}\left[\sigma_\eta^2\right], \tag{14}$$

and propose an unbiased estimator for the parametric variance using MC estimators for $\mathbb{V}ar\left[\tilde{Q}_{N_\eta}\right]$ and $\mathbb{E}_{\xi}\left[\sigma_\eta^2\right]$. To estimate the parametric variance $\mathbb{V}ar_{\xi}\left[Q\right]$ using the N_ξ samples of matrix $\boldsymbol{A}$ in Section 3, one would tally both the model output $\tilde{Q}_{N_\eta}(\boldsymbol{A})$ and the variance of the model output $\hat{\sigma}_\eta^2(\boldsymbol{A})$, then subtract the average solver variance from the total observed variance:

$$\mathbb{V}ar_{\xi}\left[Q\right] \approx S_{(A)}^2 \overset{\text{def}}{=} \tilde{S}_{(A)}^2 - \frac{1}{N_\eta}\left\langle\hat{\sigma}_\eta^2\right\rangle_{(A)}, \tag{15}$$

$$\text{where } \tilde{S}_{(A)}^2 \overset{\text{def}}{=} \frac{1}{N_\xi - 1}\sum_{v=1}^{N_\xi}\left(\tilde{Q}_{N_\eta}^2(\boldsymbol{A})_v - \left\langle\tilde{Q}_{N_\eta}\right\rangle_{(A)}^2\right), \tag{16}$$

$$\left\langle\tilde{Q}_{N_\eta}\right\rangle_{(A)} = \frac{1}{N_\xi}\sum_{v=1}^{N_\xi}\tilde{Q}_{N_\eta}(\boldsymbol{A})_v \quad \text{and} \quad \left\langle\hat{\sigma}_\eta^2\right\rangle_{(A)} = \frac{1}{N_\xi}\sum_{v=1}^{N_\xi}\hat{\sigma}_\eta^2(\boldsymbol{A}).$$

A standard approach is to estimate $\mathbb{V}ar_{\xi}\left[Q\right]$ as $\tilde{S}_{(A)}^2$, where $\tilde{S}_{(A)}^2 \to \mathbb{V}ar_{\xi}\left[Q\right]$ as $N_\eta, N_\xi \to \infty$. This standard approach is reliably accurate but computationally expensive, as large N_η is needed for each function evaluation. In [26], we showed that for the same linear computational cost $\mathbb{C} = N_\xi \times N_\eta$, $S_{(A)}^2$ was a more accurate estimate of $\mathbb{V}ar_{\xi}\left[Q\right]$ than the biased estimator $\tilde{S}_{(A)}^2$. In the next section, we extend the variance deconvolution approach to computation of Sobol' indices.

5. GSA with variance deconvolution

In this section, we first analyze how the MC estimate $\tilde{Q}_{N_\eta}$ affects the parametric sensitivity indices of Q – $\mathbb{S}_i$ and $\mathbb{T}_i$,. Then, we propose unbiased estimators for $\mathbb{S}_i$ and $\mathbb{T}_i$ using $\tilde{Q}_{N_\eta}$.

5.1. Stochastic solver's effect on sensitivity indices

We begin by considering the first- and total- order sensitivity indices of ξ_i on $\tilde{Q}_{N_\eta}$,

$$\mathbb{S}_{i,\tilde{Q}_{N_\eta}} = \frac{\mathbb{V}ar\Big[\mathbb{E}\big[\tilde{Q}_{N_\eta} \mid \xi_i\big]\Big]}{\mathbb{V}ar\left[\tilde{Q}_{N_\eta}\right]}, \tag{17}$$

$$\mathbb{T}_{i,\tilde{Q}_{N_\eta}} = \frac{\mathbb{E}\Big[\mathbb{V}ar\big[\tilde{Q}_{N_\eta} \mid \xi_{\sim i}\big]\Big]}{\mathbb{V}ar\left[\tilde{Q}_{N_\eta}\right]}. \tag{18}$$

From Eq. (14), it follows that the numerator of Eq. (17) can be simplified as

$$\begin{aligned}\mathbb{V}ar\Big[\mathbb{E}\big[\tilde{Q}_{N_\eta} \mid \xi_i\big]\Big] &= \mathbb{V}ar_{\xi_i}\Big[\mathbb{E}_{\xi_{\sim i},\eta}\big[\tilde{Q}_{N_\eta} \mid \xi_i\big]\Big] \\ &= \mathbb{V}ar_{\xi_i}\Big[\mathbb{E}_{\xi_{\sim i}}\big[Q \mid \xi_i\big]\Big]\end{aligned} \tag{19}$$

and that the numerator of Eq. (18) can be simplified as

$$\begin{aligned}
\mathbb{E}\Big[\mathbb{V}ar\big[\tilde{Q}_{N_\eta} \mid \xi_i\big]\Big] &= \mathbb{E}_{\xi_i}\Big[\mathbb{V}ar_{\xi_{\sim i},\eta}\big[\tilde{Q}_{N_\eta} \mid \xi_i\big]\Big] \\
&= \mathbb{E}_{\xi_i}\Big[\mathbb{V}ar_{\xi_{\sim i}}\big[Q \mid \xi_i\big] + \frac{1}{N_\eta}\mathbb{E}_{\xi_{\sim i}}\big[\sigma_\eta^2 \mid \xi_i\big]\Big] \\
&= \mathbb{E}_{\xi_i}\Big[\mathbb{V}ar_{\xi_{\sim i}}\big[Q \mid \xi_i\big]\Big] + \frac{1}{N_\eta}\mathbb{E}_{\xi}\left[\sigma_\eta^2\right]. \qquad (20)
\end{aligned}$$

We can therefore conclude that the first-order effect of any subset $\boldsymbol{\xi}$ on $\tilde{Q}_{N_\eta}$ is equivalent to the first-order effect of $\boldsymbol{\xi}$ on Q; however, the total-order effect of $\boldsymbol{\xi}$ on $\tilde{Q}_{N_\eta}$ is larger than the total-order effect of $\boldsymbol{\xi}$ on Q. This makes intuitive sense if we consider the meanings of the first- and total-order effects. The first-order effect of $\boldsymbol{\xi}$ on Q is the variance of Q caused exclusively by $\boldsymbol{\xi}$. As $\tilde{Q}_{N_\eta}$ is an unbiased estimator for Q, we would expect $\boldsymbol{\xi}$ to induce that same variance on $\tilde{Q}_{N_\eta}$. The total-order effect of $\boldsymbol{\xi}$ on Q is the variance of Q caused by $\boldsymbol{\xi}$ and its interactions with all remaining variables $\sim \boldsymbol{\xi}$. However, the total-order effect of $\boldsymbol{\xi}$ on $\tilde{Q}_{N_\eta}$ additionally includes the interactions of $\boldsymbol{\xi}$ with solver stochasticity η. An equivalent result was found in [35] by extending the ANOVA decomposition directly to the set of input variables $(\xi_i, \xi_{\sim i}, \eta)$.

We can write the first- and total-order sensitivity indices of ξ_i on Q in terms of $\mathbb{S}_{i,\tilde{Q}_{N_\eta}}$, $\mathbb{T}_{i,\tilde{Q}_{N_\eta}}$, and the ratio of solver variance to parametric variance $R \overset{\text{def}}{=} \frac{\mathbb{E}_\xi[\sigma_\eta^2]}{\mathbb{V}ar_\xi[Q]}$ as

$$\begin{aligned}
\mathbb{S}_{i,\tilde{Q}_{N_\eta}} &= \frac{\mathbb{V}ar_{\xi_i}\Big[\mathbb{E}_{\xi_{\sim i}}\big[Q \mid \xi_i\big]\Big]}{\mathbb{V}ar_\xi\left[Q\right] + \frac{1}{N_\eta}\mathbb{E}_\xi\left[\sigma_\eta^2\right]} \\
&\to \mathbb{S}_i = \mathbb{S}_{i,\tilde{Q}_{N_\eta}}\left(1 + \frac{R}{N_\eta}\right), \qquad (21)
\end{aligned}$$

$$\begin{aligned}
\mathbb{T}_{i,\tilde{Q}_{N_\eta}} &= \frac{\mathbb{E}_{\xi_{\sim i}}\Big[\mathbb{V}ar_{\xi_i}\big[Q \mid \xi_{\sim i}\big]\Big] + \frac{1}{N_\eta}\mathbb{E}_\xi\left[\sigma_\eta^2\right]}{\mathbb{V}ar_\xi\left[Q\right] + \frac{1}{N_\eta}\mathbb{E}_\xi\left[\sigma_\eta^2\right]} \\
&\to \mathbb{T}_i = \mathbb{T}_{i,\tilde{Q}_{N_\eta}}\left(1 + \frac{R}{N_\eta}\right) - \frac{R}{N_\eta}. \qquad (22)
\end{aligned}$$

From Equations (21) and (22), it is clear that the sets of indices $\left(\mathbb{S}_{i,\tilde{Q}_{N_\eta}}, \mathbb{T}_{i,\tilde{Q}_{N_\eta}}\right)$ and $(\mathbb{S}_i, \mathbb{T}_i)$ are not equivalent. Unlike the relationship among $\mathbb{V}ar\left[\tilde{Q}_{N_\eta}\right]$, $\mathbb{V}ar_\xi\left[Q\right]$, and $\mathbb{E}\left[\sigma_\eta^2\right]$, the relationships between the SIs of $\tilde{Q}_{N_\eta}$ and Q are not simply additive. Because $R \geq 0$, $\mathbb{S}_{i,\tilde{Q}_{N_\eta}}$ will always be *less than* $\mathbb{S}_i$ and underestimate the first-order effect of ξ_i. On the other hand, $\mathbb{T}_{i,\tilde{Q}_{N_\eta}}$ will always be *greater than* $\mathbb{T}_i$ and overestimate the total-order effect of ξ_i.

Substituting $\tilde{Q}_{N_\eta}$ for Q in Equations (12) and (13) will yield unbiased estimates of $\mathbb{S}_{i,\tilde{Q}_{N_\eta}}$ and $\mathbb{T}_{i,\tilde{Q}_{N_\eta}}$, not of $\mathbb{S}_i$ and $\mathbb{T}_i$, although both $\mathbb{S}_{i,\tilde{Q}_{N_\eta}}$ and $\mathbb{T}_{i,\tilde{Q}_{N_\eta}}$ will approach their parametric counterparts in the limit $N_\eta = \infty$. Because we desire estimates of $\mathbb{S}_i$ and $\mathbb{T}_i$, we extend the variance deconvolution framework to propose unbiased sampling estimators for $\mathbb{S}_i$ and $\mathbb{T}_i$ using $\tilde{Q}_{N_\eta}$ by introducing terms to correct biases in $\mathbb{S}_{i,\tilde{Q}_{N_\eta}}$ and $\mathbb{T}_{i,\tilde{Q}_{N_\eta}}$.

5.2. *Unbiased sampling estimators using $\tilde{Q}_{N_\eta}$*

For unbiased estimates of $\mathbb{S}_i$ and $\mathbb{T}_i$ from $\tilde{Q}_{N_\eta}$, the denominator of $\mathbb{S}_{i,\tilde{Q}_{N_\eta}}$ in Eq. (21) and both the numerator and denominator of $\mathbb{T}_{i,\tilde{Q}_{N_\eta}}$ in Eq. (22) require a corrective term. It is possible that this varies from estimator-to-estimator; in short, terms that require a $\hat{\sigma}_\eta^2$ correction arise when $\tilde{Q}_{N_\eta}(\boldsymbol{\xi})$ is squared, but not when two independent realizations of $\tilde{Q}_{N_\eta}$ are multiplied, e.g., $\tilde{Q}_{N_\eta}(\boldsymbol{B})_v \tilde{Q}_{N_\eta}(\boldsymbol{A}_{\boldsymbol{B}}^{(i)})_v$.

To understand the impact of introducing a corrective variance deconvolution term, we consider two sets of estimators that use $\tilde{Q}_{N_\eta}$ – "standard" and variance deconvolution. The "standard" estimators $\hat{\mathbb{S}}_i^{St.}$ and $\hat{\mathbb{T}}_i^{St.}$ result from inserting $\tilde{Q}_{N_\eta}$ directly into the estimators in Eq. (21) and Eq. (22). The variance deconvolution estimators $\hat{\mathbb{S}}_i^{Va.}$ and $\hat{\mathbb{T}}_i^{Va.}$ result from introducing corrective $\hat{\sigma}_\eta^2$ terms into the standard estimators.

The standard estimators are:

$$\hat{\mathbb{S}}_i^{St.} \stackrel{\text{def}}{=} \frac{\frac{1}{N_\xi}\sum_{v=1}^{N_\xi} \tilde{Q}_{N_\eta}(\boldsymbol{B})_v \left[\tilde{Q}_{N_\eta}(\boldsymbol{A}_{\boldsymbol{B}}^{(\boldsymbol{i})})_v - \tilde{Q}_{N_\eta}(\boldsymbol{A})_v\right]}{\frac{1}{2N_\xi}\sum_{v=1}^{N_\xi}\left(\tilde{Q}_{N_\eta}(\boldsymbol{A})_v - \tilde{Q}_{N_\eta}(\boldsymbol{B})_v\right)^2} \stackrel{\text{def}}{=} \frac{\hat{\mathbb{V}}_i^{St.}}{\tilde{S}^2_{(AB)}}, \tag{23}$$

$$\hat{\mathbb{T}}_i^{St.} \stackrel{\text{def}}{=} \frac{\frac{1}{2N_\xi}\left[\tilde{Q}_{N_\eta}(\boldsymbol{A}_{\boldsymbol{B}}^{(\boldsymbol{i})})_v - \tilde{Q}_{N_\eta}(\boldsymbol{A})_v\right]^2}{\frac{1}{2N_\xi}\sum_{v=1}^{N_\xi}\left(\tilde{Q}_{N_\eta}(\boldsymbol{A})_v - \tilde{Q}_{N_\eta}(\boldsymbol{B})_v\right)^2} \stackrel{\text{def}}{=} \frac{\hat{\mathbb{E}}_{\sim i}^{St.}}{\tilde{S}^2_{(AB)}}. \tag{24}$$

The variance deconvolution estimators follow from Eqs. (21) and (22),

$$\mathbb{S}_i \approx \hat{\mathbb{S}}_i^{Va.} \stackrel{\text{def}}{=} \frac{\hat{\mathbb{V}}_i^{St.}}{\tilde{S}^2_{(AB)} - \frac{1}{N_\eta}\left\langle \hat{\sigma}_\eta^2 \right\rangle_{(AB)}} \quad \text{and} \tag{25}$$

$$\mathbb{T}_i \approx \hat{\mathbb{T}}_i^{Va.} \stackrel{\text{def}}{=} \frac{\hat{\mathbb{E}}_{\sim i}^{St.} - \frac{1}{N_\eta}\left\langle \hat{\sigma}_\eta^2 \right\rangle_{(A_B^i A)}}{\tilde{S}^2_{(AB)} - \frac{1}{N_\eta}\left\langle \hat{\sigma}_\eta^2 \right\rangle_{(AB)}}, \tag{26}$$

where

$$\left\langle \hat{\sigma}_\eta^2 \right\rangle_{(AB)} \stackrel{\text{def}}{=} \frac{1}{2N_\xi}\sum_{v=1}^{N_\xi}\left[\hat{\sigma}_\eta^2(\boldsymbol{A})_v + \hat{\sigma}_\eta^2(\boldsymbol{B})_v\right]. \tag{27}$$

The additional variance deconvolution terms are introduced to correct the noise introduction from the stochastic solver while keeping consistent with the construction of the existing estimators; specifically, the numerator and denominator of $\hat{\mathbb{T}}_i^{Va.}$ require different average solver noise terms because $\hat{\mathbb{E}}_i^{St.}$ contains $\tilde{Q}_{N_\eta}(A_B^i)$ squared while $\tilde{S}^2_{(AB)}$ contains $\tilde{Q}_{N_\eta}(A)$ squared. We would also expect the behavior of the variance deconvolution estimators to be consistent with that of the existing estimators; for example, this set of estimators $\hat{\mathbb{S}}_i$ and $\hat{\mathbb{T}}_i$ does not guarantee that $\hat{\mathbb{T}}_i \geq \hat{\mathbb{S}}_i$ [66]; we would expect to see that same behavior with the variance deconvolution versions of these estimators. In the next section, we compare the statistical properties of the standard and variance-deconvolution estimators.

5.3. Mean-squared error of the estimators

The performance of an estimator $\hat{\theta}$ for true value θ is characterized by mean-squared error, which captures both its *variance* and *bias*:

$$\begin{aligned} MSE\left[\hat{\theta}\right] &= \mathbb{V}ar\left[\hat{\theta}\right] + \left(\mathbb{E}\left[\hat{\theta}\right] - \theta\right)^2 \\ &= \mathbb{V}ar\left[\hat{\theta}\right] + \mathbb{B}ias^2\left[\hat{\theta}, \theta\right]. \end{aligned}$$

An *unbiased* estimator will on average yield the true values of the Sobol' indices, and an estimator with small variance will on average yield values that remain close to its average [66]. In Appendix A, we establish the variances and biases of the standard and variance-deconvolution estimators under the asymptotic normality assumption [67, 51, 66].

They are, respectively,

$$\mathbb{B}ias^2\left[\hat{\mathbb{S}}_i^{St.}, \mathbb{S}_i\right] = \frac{\mathbb{S}_i^2}{N_\eta{}^2}\frac{\mathbb{E}_\xi^2\left[\sigma_\eta^2\right]}{\mathbb{V}ar^2\left[\tilde{Q}_{N_\eta}\right]} \tag{28}$$

$$\mathbb{B}ias^2\left[\hat{\mathbb{S}}_i^{Va.}, \mathbb{S}_i\right] = 0 \tag{29}$$

$$\mathbb{B}ias^2\left[\hat{\mathbb{T}}_i^{St.}, \mathbb{T}_i\right] = \frac{\mathbb{T}_i^2}{N_\eta{}^2}\frac{\mathbb{E}_\xi^2\left[\sigma_\eta^2\right]\mathbb{V}_{\sim i}^2}{\mathbb{V}ar^2\left[\tilde{Q}_{N_\eta}\right]\mathbb{E}_{\sim i}^2} \tag{30}$$

$$\mathbb{B}ias^2\left[\hat{\mathbb{T}}_i^{Va.}, \mathbb{T}_i\right] = 0, \tag{31}$$

and,

$$\begin{aligned}\mathbb{V}ar\left[\hat{\mathbb{S}}_i^{St.}\right] = \frac{1}{\mathbb{V}ar^2\left[\tilde{Q}_{N_\eta}\right]}\mathbb{V}ar\Bigg[&\tilde{Q}_{N_\eta}(\boldsymbol{B})\left(\tilde{Q}_{N_\eta}(\boldsymbol{A}_{\boldsymbol{B}}^{(i)}) - \tilde{Q}_{N_\eta}(\boldsymbol{A})\right) \\ &- \mathbb{S}_i\frac{\mathbb{V}ar_\xi\left[Q\right]}{2\mathbb{V}ar\left[\tilde{Q}_{N_\eta}\right]}\left(\tilde{Q}_{N_\eta}(\boldsymbol{A}) - \tilde{Q}_{N_\eta}(\boldsymbol{B})\right)^2\Bigg]\end{aligned} \tag{32}$$

$$\begin{aligned}\mathbb{V}ar\left[\hat{\mathbb{S}}_i^{Va.}\right] = \frac{1}{\mathbb{V}ar_\xi^2\left[Q\right]}\mathbb{V}ar\Bigg[&\tilde{Q}_{N_\eta}(\boldsymbol{B})\left(\tilde{Q}_{N_\eta}(\boldsymbol{A}_{\boldsymbol{B}}^{(i)}) - \tilde{Q}_{N_\eta}(\boldsymbol{A})\right) \\ &- \mathbb{S}_i\frac{1}{2}\left(\tilde{Q}_{N_\eta}(\boldsymbol{A}) - \tilde{Q}_{N_\eta}(\boldsymbol{B})\right)^2 \\ &+ \mathbb{S}_i\frac{1}{2N_\eta}\left(\hat{\sigma}_\eta^2(A) + \hat{\sigma}_\eta^2(B)\right)\Bigg]\end{aligned} \tag{33}$$

$$\begin{aligned}\mathbb{V}ar\left[\hat{\mathbb{T}}_i^{St.}\right] = \frac{1}{\mathbb{V}ar^2\left[\tilde{Q}_{N_\eta}\right]}\mathbb{V}ar\Bigg[&\frac{1}{2}\left(\tilde{Q}_{N_\eta}(\boldsymbol{A}_{\boldsymbol{B}}^{(i)}) - \tilde{Q}_{N_\eta}(\boldsymbol{A})\right)^2 \\ &- \mathbb{T}_i\frac{\mathbb{V}ar_\xi\left[Q\right]\mathbb{E}_{\sim i,\tilde{Q}_{N_\eta}}}{2\mathbb{V}ar\left[\tilde{Q}_{N_\eta}\right]\mathbb{E}_{\sim i}}\left(\tilde{Q}_{N_\eta}(\boldsymbol{A}) - \tilde{Q}_{N_\eta}(\boldsymbol{B})\right)^2\Bigg]\end{aligned} \tag{34}$$

$$\begin{aligned}\mathbb{V}ar\left[\hat{\mathbb{T}}_i^{Va.}\right] = \frac{1}{\mathbb{V}ar_\xi^2\left[Q\right]}\mathbb{V}ar\Bigg[&\frac{1}{2}\left(\tilde{Q}_{N_\eta}(\boldsymbol{A}_{\boldsymbol{B}}^{(i)}) - \tilde{Q}_{N_\eta}(\boldsymbol{A})\right)^2 - \frac{1}{2N_\eta}\left(\hat{\sigma}_\eta^2(\boldsymbol{A}_{\boldsymbol{B}}^{\boldsymbol{i}}) + \hat{\sigma}_\eta^2(\boldsymbol{A})\right) \\ &- \mathbb{T}_i\left(\frac{1}{2}\left(\tilde{Q}_{N_\eta}(\boldsymbol{A}) - \tilde{Q}_{N_\eta}(\boldsymbol{B})\right)^2 - \frac{1}{2N_\eta}\left(\hat{\sigma}_\eta^2(\boldsymbol{A}) + \hat{\sigma}_\eta^2(\boldsymbol{B})\right)\right)\Bigg].\end{aligned} \tag{35}$$

When variance deconvolution is applied to $\mathbb{V}ar\left[\tilde{Q}_{N_\eta}\right]$ to develop the unbiased estimator $\mathbb{V}ar_\xi\left[Q\right] \approx S^2 = \tilde{S}^2 - \frac{1}{N_\eta}\left\langle\hat{\sigma}_\eta^2\right\rangle$, the additive relationship gives rise to a simple bias term $\frac{1}{N_\eta}\left\langle\hat{\sigma}_\eta^2\right\rangle$ and relatively simple variance $\mathbb{V}ar\left[S^2\right] = \mathbb{V}ar\left[\tilde{S}^2\right] + \frac{1}{N_\eta{}^2}\mathbb{V}ar\left[\left\langle\hat{\sigma}_\eta^2\right\rangle\right] - \frac{2}{N_\eta}\mathbb{C}ov\left[\tilde{S}^2, \left\langle\hat{\sigma}_\eta^2\right\rangle\right]$ [26]. Because the SI estimators are ratios, the relationships between $\left(\mathbb{S}_i, \mathbb{S}_{i,\tilde{Q}_{N_\eta}}\right)$ and $\left(\mathbb{T}_i, \mathbb{T}_{i,\tilde{Q}_{N_\eta}}\right)$ are not simply additive and their variances are less straightforward to compare. The variance deconvolution estimators are unbiased; the biases of the standard estimators are functions of N_η, the magnitude of the SIs, and the ratio of the solver noise to the total observed variance. Notably, the biases are larger for larger index values.

It is less obvious to draw comparisons between the variances of $\left(\hat{\mathbb{S}}_i^{Va.}, \hat{\mathbb{S}}_i^{St.}\right)$ and $\left(\hat{\mathbb{T}}_i^{Va.}, \hat{\mathbb{T}}_i^{St.}\right)$. In particular, because a correction term is necessary in both the numerator and denominator of $\mathbb{T}_i$, its estimators' biases and variances are more complex than their $\mathbb{S}_i$ counterparts. We investigate the statistics of the estimators in the next section through numerical simulation.

6. Numerical results

In this section, we illustrate the performance of the standard and variance deconvolution Saltelli SI estimators. We first discuss results for a common GSA numerical example – the Ishigami function. Then, we test the method on a Monte Carlo radiation transport problem.

We consider the Ishigami function [42] as a case in which the true solution for $Q(\xi)$, $\mathbb{V}ar_{\xi}[Q]$, and the full set of first- and total-order estimators is known:

$$Q(\xi) = \sin(\xi_1) + 7\sin^2(\xi_2) + 0.1\xi_3^4\sin(\xi_1), \tag{36}$$

where the input parameters are independently uniformly distributed over $[-\pi, \pi]$. We introduce stochasticity to the problem by adding a random variable $\eta \sim \mathcal{N}[0,1]$ multiplied by a constant,

$$f(\xi, \eta) = Q(\xi) + c\eta, \tag{37}$$

and approximate $Q(\xi)$ as $\tilde{Q}_{N_\eta}(\xi)$ using MC. This results in a total variance

$$\mathbb{V}ar\left[\tilde{Q}_{N_\eta}\right] = \mathbb{V}ar_{\xi}[Q] + \frac{c^2}{N_\eta}, \tag{38}$$

where $\mathbb{V}ar_{\xi}[Q] = 13.84$ is the known variance of the Ishigami function. The expected value of the Ishigami function is $\mathbb{E}_{\xi}[Q] = 3.5$. The behavior of the Ishigami indices is also known: ξ_1 and ξ_3 are highly interactive while ξ_2 is purely additive, i.e., $\mathbb{S}_2 = \mathbb{T}_2$, and $\mathbb{S}_3 = 0$. This allows us to observe the behavior of the variance deconvolution estimators under both purely additive and highly-interactive model conditions, as well as their behavior when an index is equal to zero, which can cause estimator performance to suffer. In this exercise, we numerically compare the performance of the standard estimators (Eqs. (23) and (24)) with the performance of the variance deconvolution estimators (Eqs. (25) and (26)). Changing the constant c allows us to control how much the solver noise contributes to the total variance and how much resolution is needed in N_η. We compare their behavior for multiple combinations of (N_ξ, N_η) and replicate one hundred estimates of the first- and total-order indices using the procedure laid out in Section 3. We note again that we are sampling the parameter space using purely random MC.

6.0.1. Equal solver and parameter noise

We first consider the case in which $c = 3.721$, such that the solver noise contributes about 50% of the variance of a single tally f. In Figures 1 and 2, we show boxplots of the 100 replicates of first- and total-order Sobol' indices (respectively), where the boxplot represents the minimum, first-quartile, median, third-quartile and maximum, plus the mean in a dotted line. We see that the solver noise has been resolved out with $N_\eta = 100$ solver samples and the standard and variance deconvolution estimators have both converged to the true indices with similar variances. For the boxplots in Figures 3 and 4, we have reduced the solver sample size to $N_\eta = 2$, a 50X reduction in total cost. For $\mathbb{S}_1$ and $\mathbb{S}_2$, we see that the variance deconvolution estimator has a similar spread as the standard estimator, but the standard estimator's bias is such that the true value is outside the first quartile. As predicted, the bias of the standard estimator underestimates the true first-order indices. Both estimators accurately find $\mathbb{S}_3 = 0$, however, we see that the variance deconvolution estimator has a larger variability than the standard estimator. For all three total-order indices, the bias of the standard estimator overestimates the true indices; for $\mathbb{T}_2$ and $\mathbb{T}_3$, the true value is entirely outside of the boxplot. The decrease in computational cost did affect the variance deconvolution estimator; for $\mathbb{T}_1$ in particular, we see that while the variance deconvolution estimator is unbiased, its variability is has increased and is larger than that of the standard estimator. In $\mathbb{T}_3$, we see that the low-resolution estimate of the solver variance has caused the variance deconvolution to, in essence, over-correct.

6.0.2. Solver noise is double parameter noise

We now consider the case in which $c = 5.3$, such that the solver noise contributes about 67% of the variance of a single tally f. In this case, more solver samples are required to produce unbiased indices using the standard estimators; in Figures 5 and 6, $N_\eta = 500$ were used, producing nearly identical results from the standard and variance deconvolution estimators.

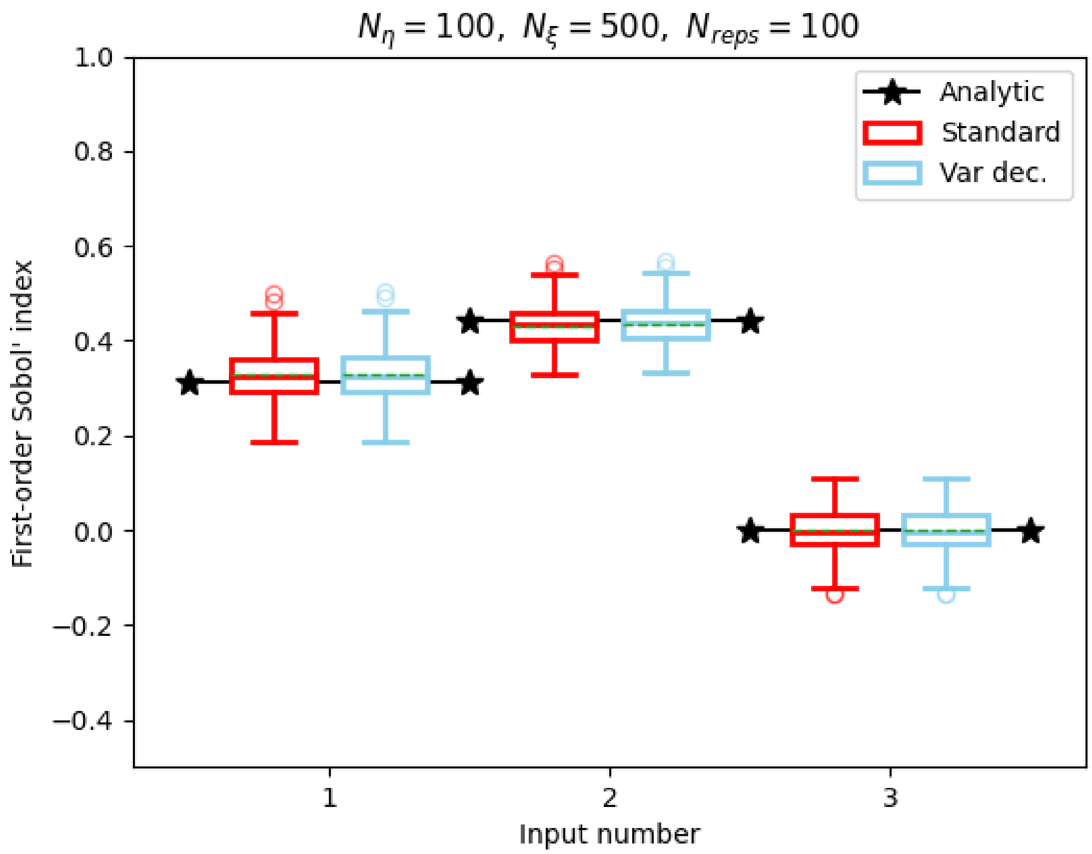

Figure 1: Boxplot of the 100 replicates of first-order Sobol' indices, where the solver noise is approx. equal to the parameter noise. The boxplot represents the minimum, first-quartile, median, third-quartile and maximum, plus the mean with a dotted line.

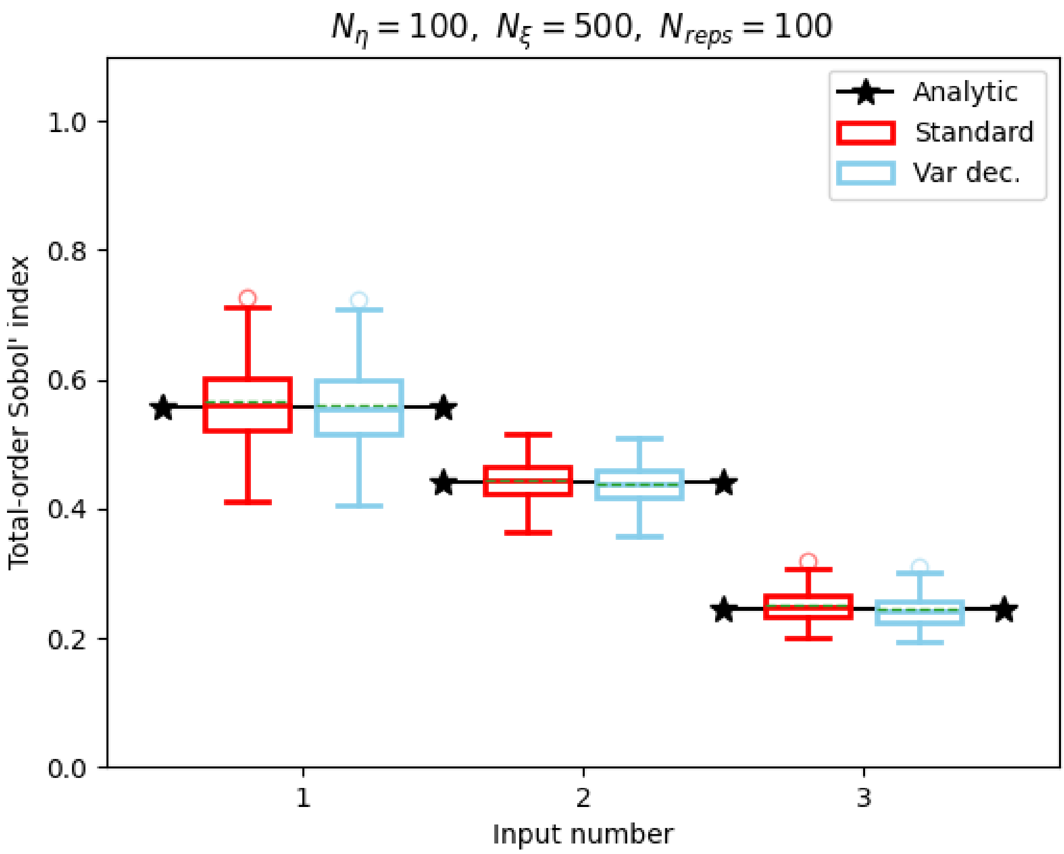

Figure 2: Boxplot of the 100 replicates of first-order Sobol' indices, where the solver noise is approx. equal to the parameter noise. The boxplot represents the minimum, first-quartile, median, third-quartile and maximum, plus the mean with a dotted line.

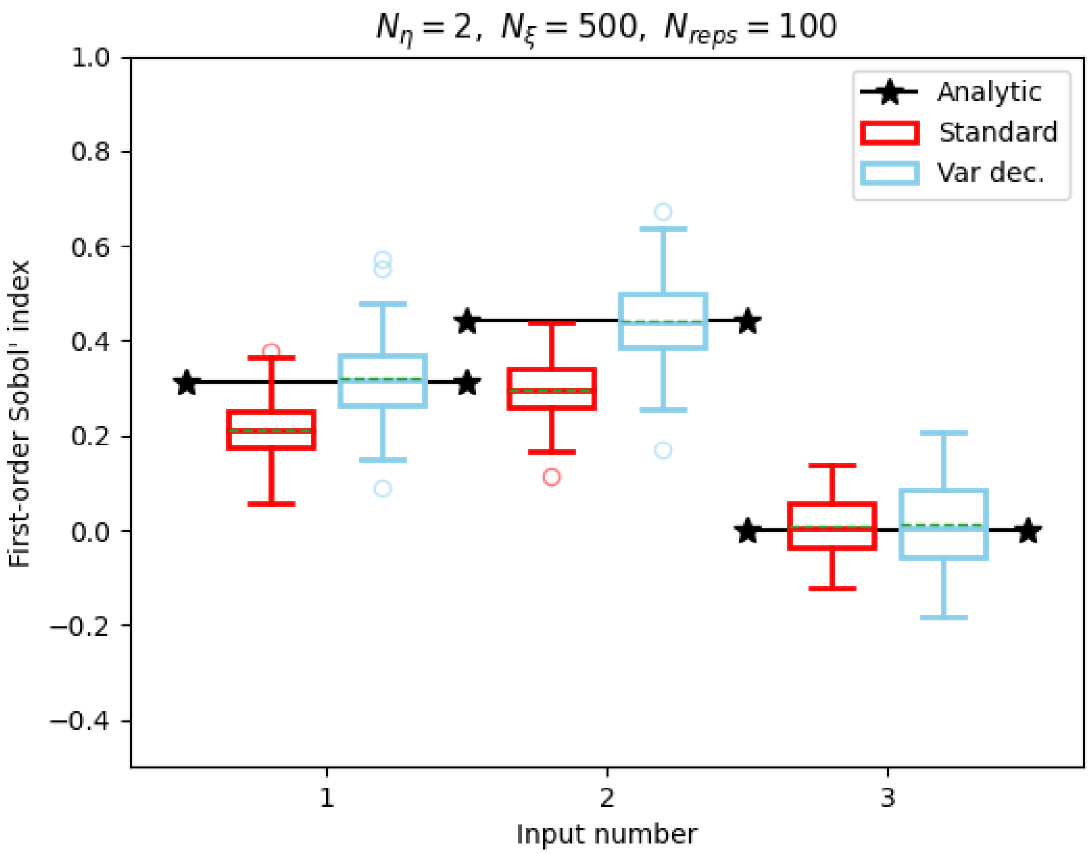

Figure 3: Boxplot of the 100 replicates of first-order Sobol' indices, where the solver noise is approx. equal to the parameter noise. The boxplot represents the minimum, first-quartile, median, third-quartile and maximum, plus the mean with a dotted line.

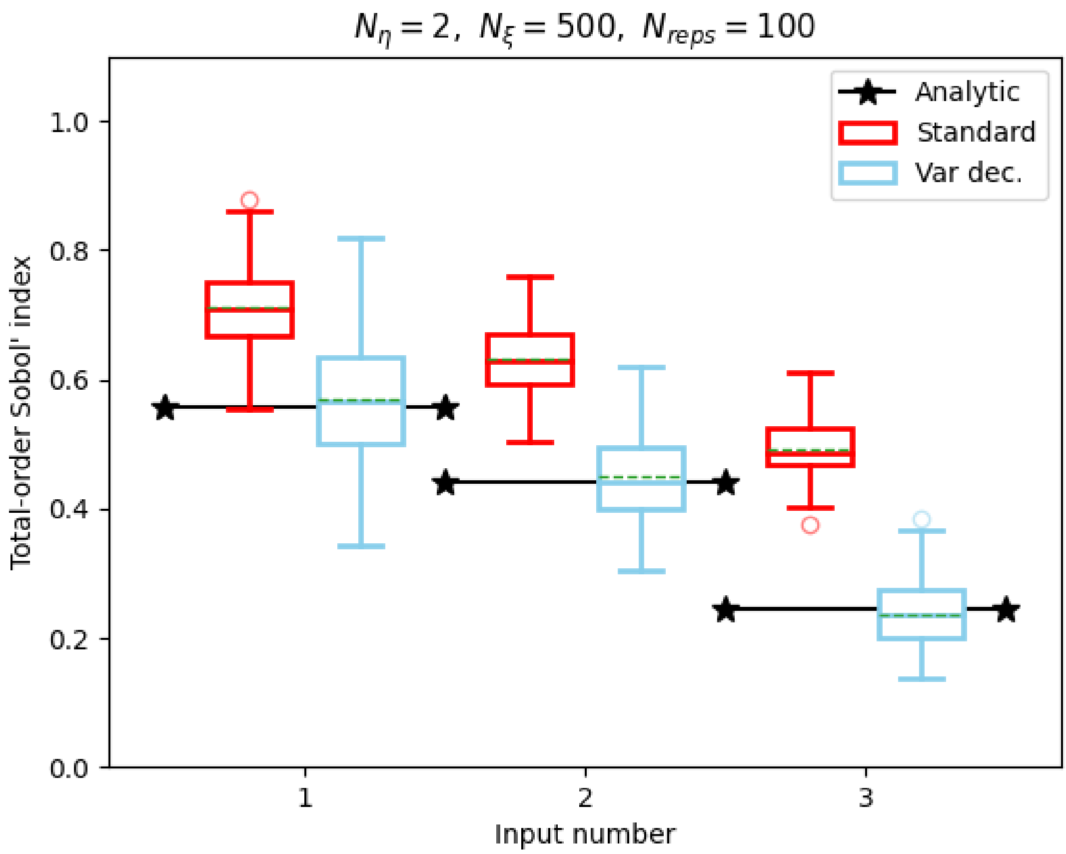

Figure 4: Boxplot of the 100 replicates of first-order Sobol' indices, where the solver noise is approx. equal to the parameter noise. The boxplot represents the minimum, first-quartile, median, third-quartile and maximum, plus the mean with a dotted line.

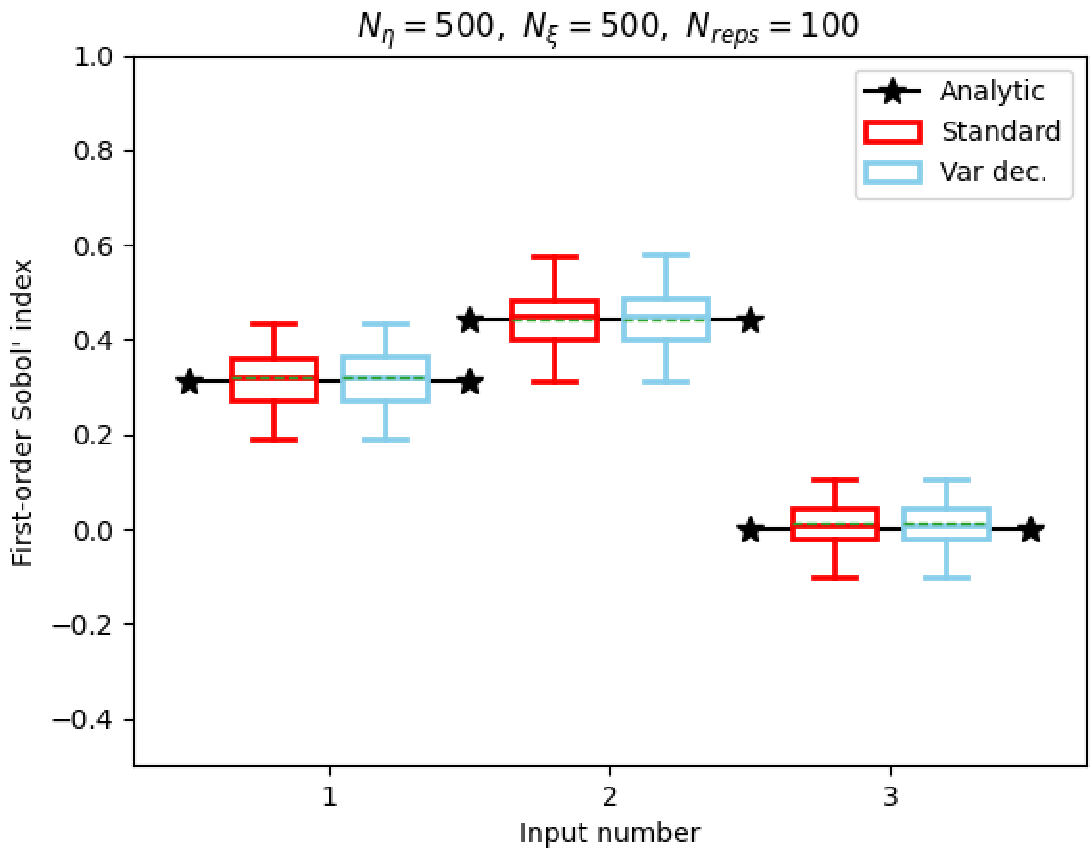

Figure 5: Boxplot of the 100 replicates of first-order Sobol' indices, where the solver noise is approx. double the parameter noise. The boxplot represents the minimum, first-quartile, median, third-quartile and maximum, plus the mean with a dotted line.

In Figures 7 and 8, we again use the minimum number of solver samples $N_\eta = 2$, now a 250X reduction in cost. This produces large biases in the standard estimator and large variabilities and some over-correction in the variance deconvolution estimator.

Finally, in Figures 9 and 10, we use $N_\eta = 10$ solver samples, a 50X reduction from the well-resolved $N_\eta = 500$. The variance deconvolution estimator is no longer over-correcting and is accurately computing all indices with a variability similar to that of the standard estimator. For all indices except $\mathbb{S}_3$, bias is still largely affecting the standard estimator.

6.1. Radiation transport test problem

We next perform GSA on a contrived neutron transport problem solved using Monte Carlo radiation transport methods [68]. The problem is one-dimensional in space and steady-state in time, with the neutron energy spectrum is divided into 7 energy groups. The problem has three components that make up a repeating lattice: a spatially-homogenized uranium dioxide (UO_2) fuel pin, water moderator, and a spatially homogenized control rod. There is an isotropic source, uniform in energy across all groups, at the spatial halfway point. We use multi-group cross sections and geometry specifications from C5G7, a nuclear reactor benchmark developed by OECD/NEA [69]. In recent work, we tested the developed estimators on the full two-dimensional C5G7 benchmark; for more detail, see [**?**].

To test a wide spectrum of physics behavior, we introduce large parameter uncertainty to five independent factors. The densities of the fuel (1), the moderator (2), and the control rod (3) vary uniformly ±70% around their respective means; the ratio of fuel-diameter to moderator-diameter (4) ; and the diameter of the control rod (5) varies uniformly

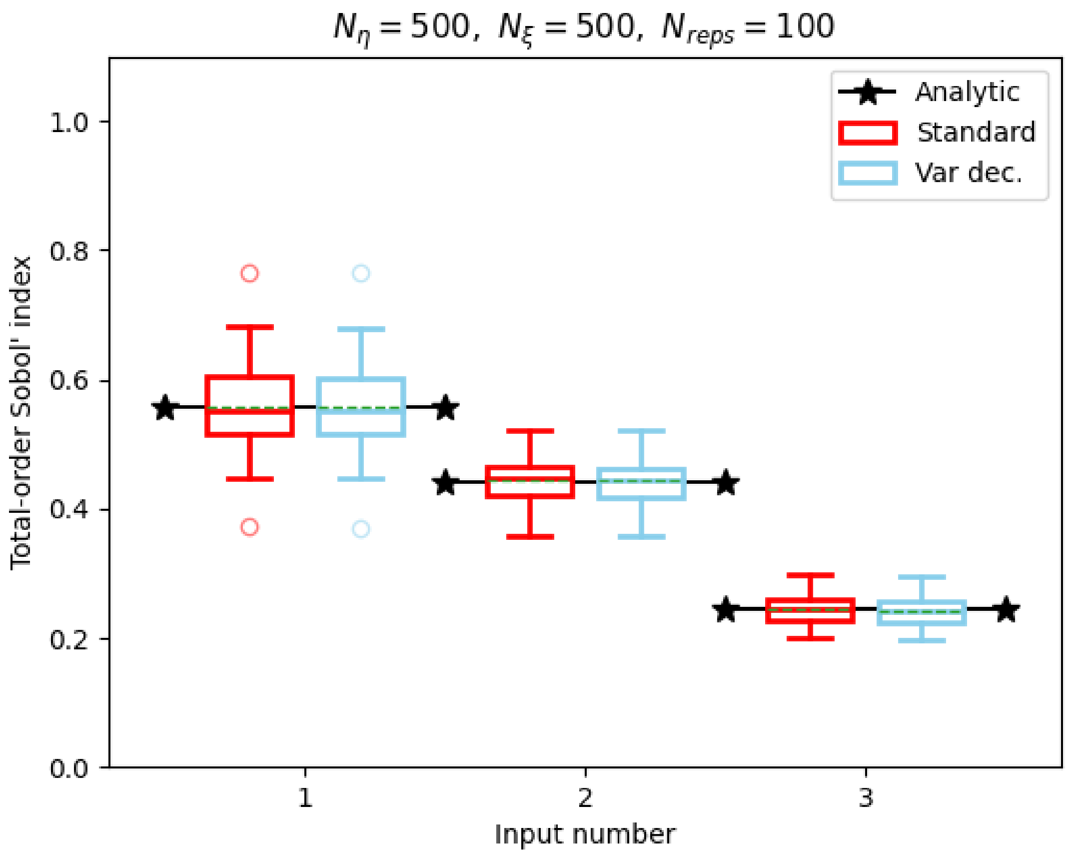

Figure 6: Boxplot of the 100 replicates of first-order Sobol' indices, where the solver noise is approx. double the parameter noise. The boxplot represents the minimum, first-quartile, median, third-quartile and maximum, plus the mean with a dotted line.

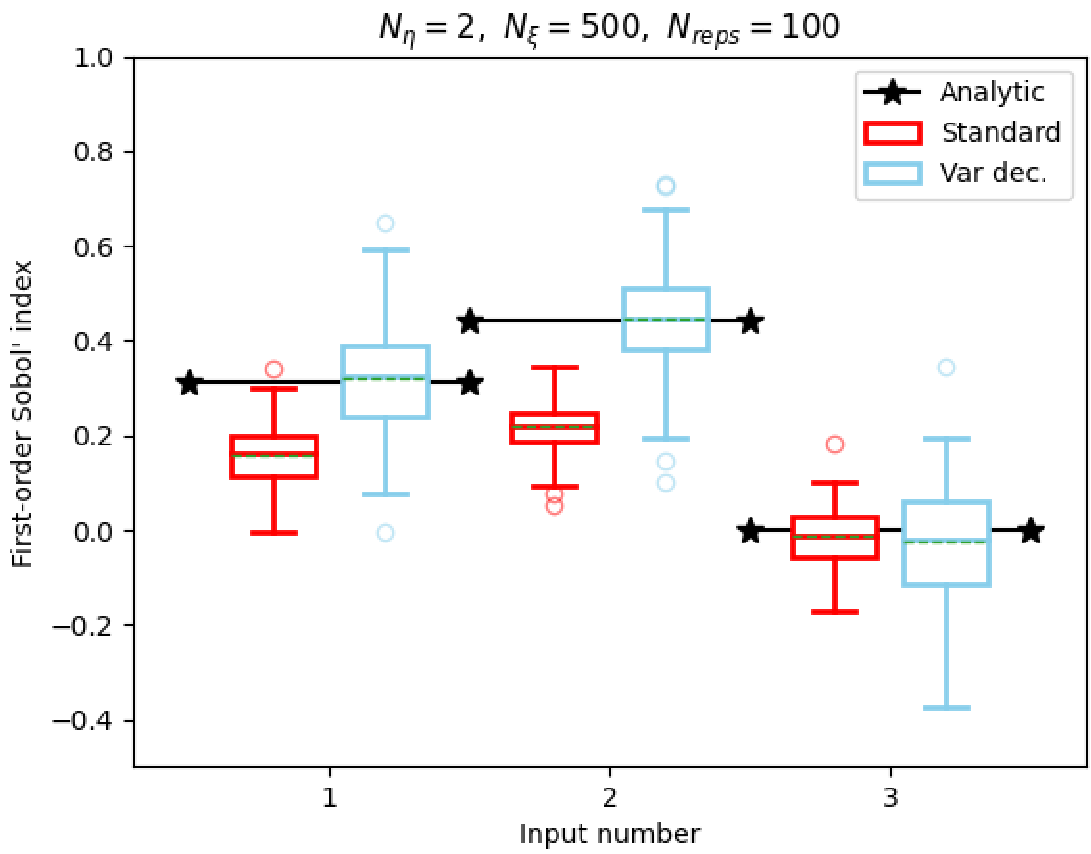

Figure 7: Boxplot of the 100 replicates of first-order Sobol' indices, where the solver noise is approx. double the parameter noise. The boxplot represents the minimum, first-quartile, median, third-quartile and maximum, plus the mean with a dotted line.

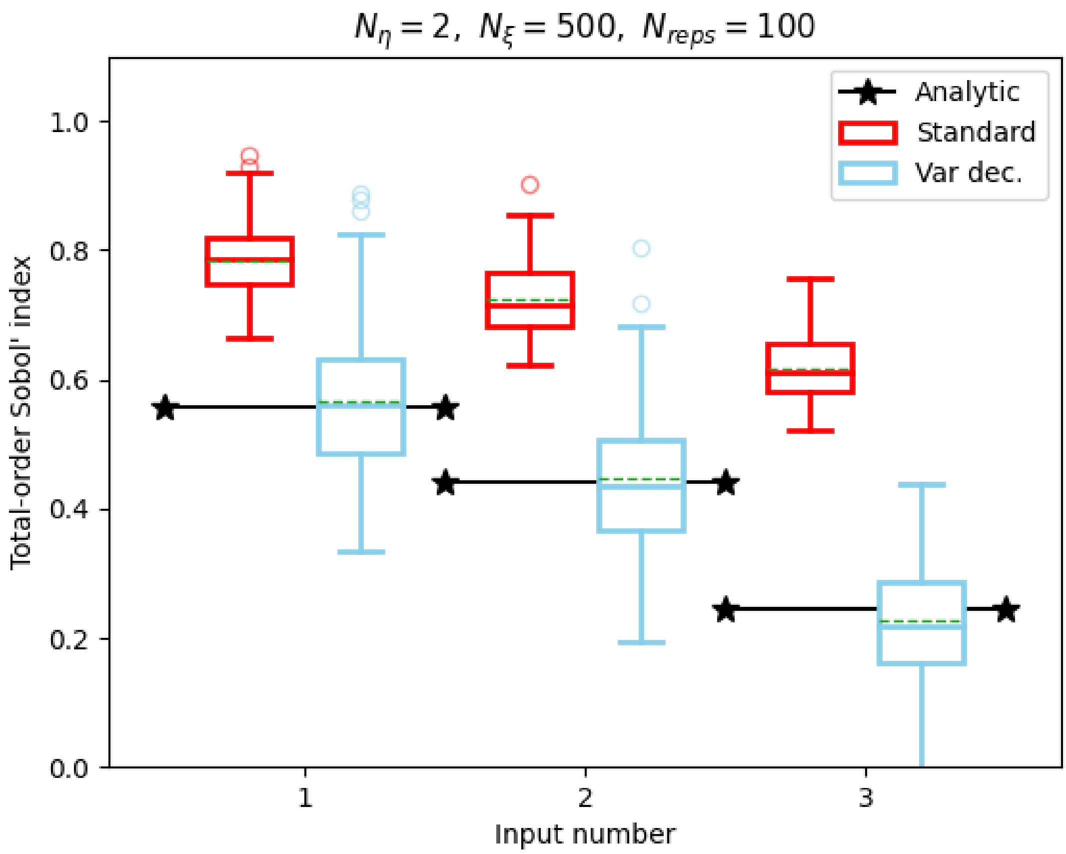

Figure 8: Boxplot of the 100 replicates of first-order Sobol' indices, where the solver noise is approx. double the parameter noise. The boxplot represents the minimum, first-quartile, median, third-quartile and maximum, plus the mean with a dotted line.

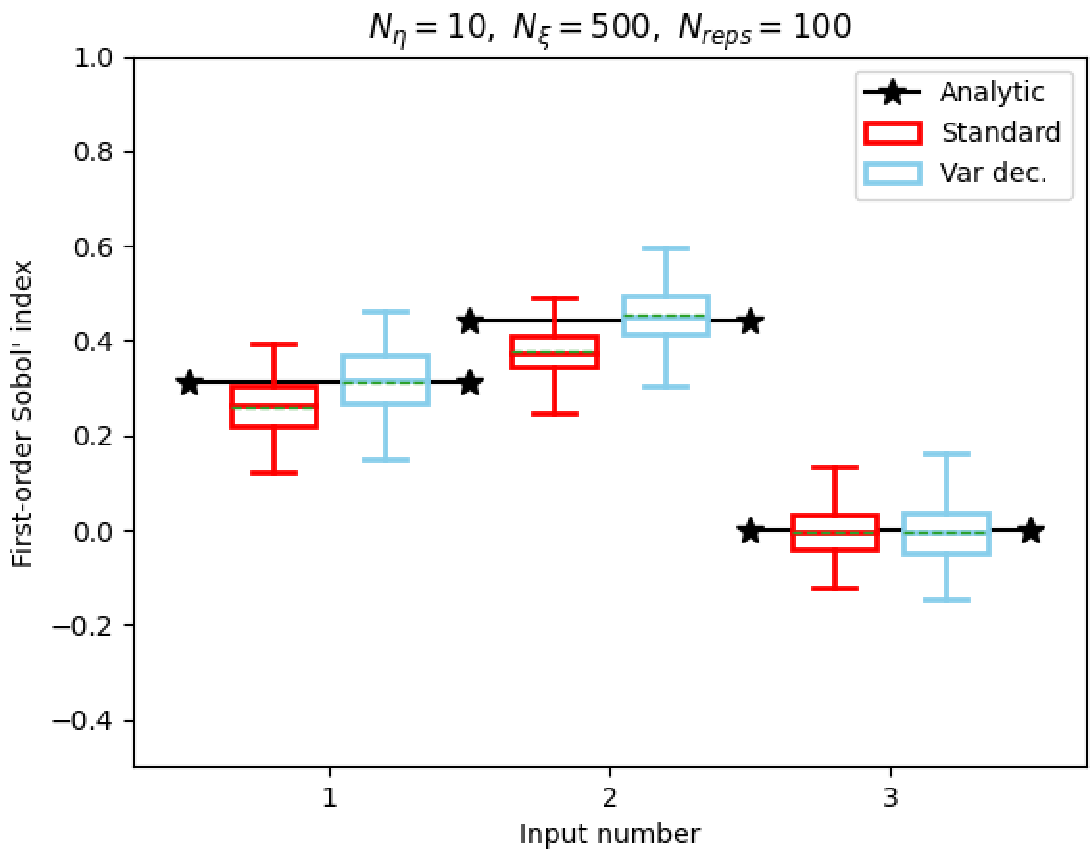

Figure 9: Boxplot of the 100 replicates of first-order Sobol' indices, where the solver noise is approx. double the parameter noise. The boxplot represents the minimum, first-quartile, median, third-quartile and maximum, plus the mean with a dotted line.

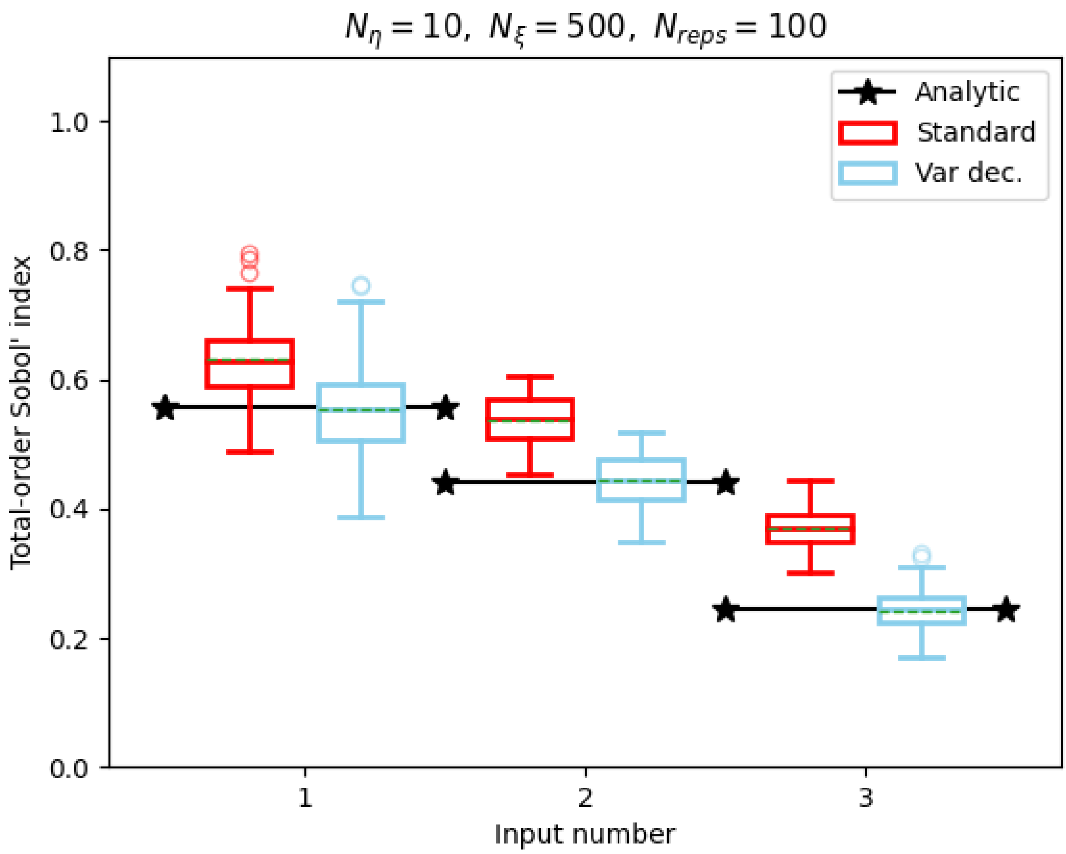

Figure 10: Boxplot of the 100 replicates of first-order Sobol' indices, where the solver noise is approx. double the parameter noise. The boxplot represents the minimum, first-quartile, median, third-quartile and maximum, plus the mean with a dotted line.

between 0.2 and 0.8. We define two quantities of interest as a function of space: the scalar flux integrated over the first two energy groups $\phi_F(x)$, and the scalar flux integrated over the remaining five energy groups $\phi_S(x)$.

For reference, using $N_\xi = 5 \times 10^5$ and $N_\eta = 10^5$, Figure 11 shows $\phi_F(x)$ and $\phi_S(x)$. Figure 12 shows the full set of first- and total-order indices for both QoIs. At this high N_η, as expected, we see that $\hat{\mathbb{S}}_i^{St.}$ and $\hat{\mathbb{T}}_i^{St.}$ converge respectively to $\hat{\mathbb{S}}_i^{Va.}$ and $\hat{\mathbb{T}}_i^{Va.}$, causing their lines to overlap. The faster group flux ϕ_F is most sensitive throughout the spatial domain to the density of the moderator (ξ_2), which is understandable as the density of the moderator will greatly impact the number of neutrons and their energies everywhere in the problem. The control rod's density (ξ_3) and thickness (ξ_5) are most impactful for the slower group flux, $\phi_S(x)$, with both having large inflection points at the nominal moderator–control rod boundary at $x = 1.5$. This is understandable, as the control rod is a primarily thermal absorber.

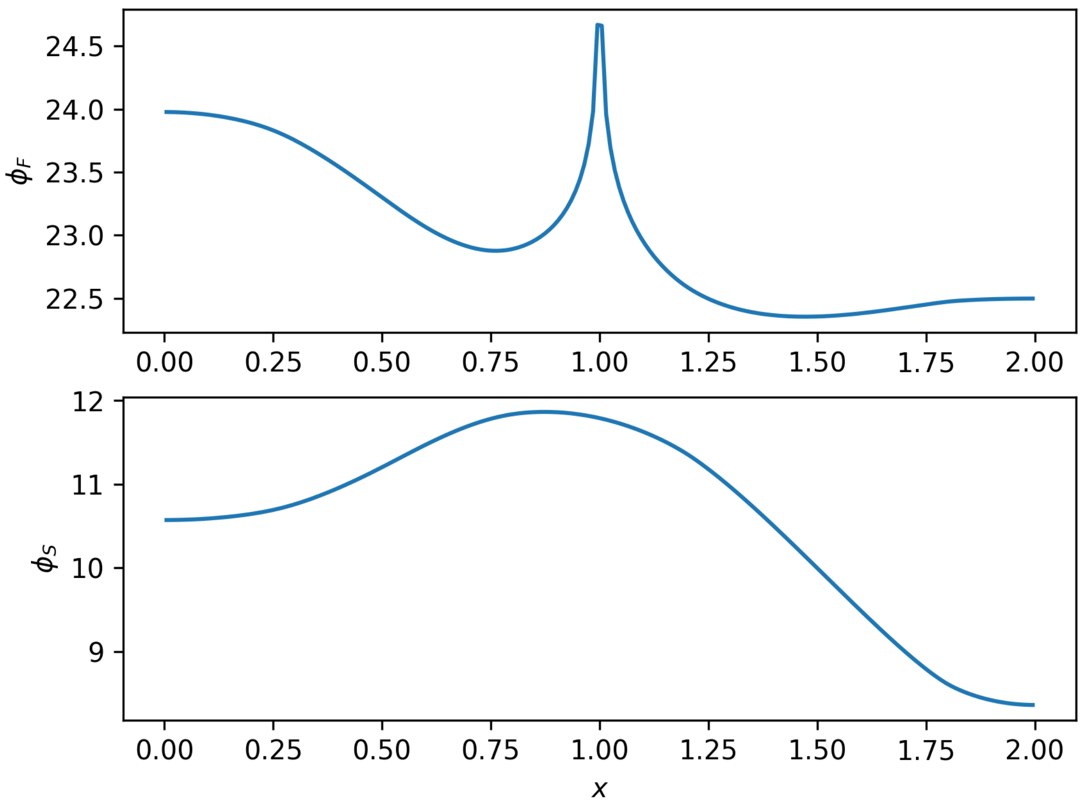

Figure 11: Average scalar flux with five uncertain parameters using $N_\xi = 5 \times 10^5$, $N_\eta = 10^5$.

To see the effect of the variance deconvolution correction, we compare the MSE of the standard and corrected estimators. In Figure 13, we consider a constant computational cost $C = \left(N_\xi \times N_\eta\right) = 5 \times 10^5$ in two different combinations of N_ξ and N_η. In the first combination, $\left(N_\xi, N_\eta\right) = \left(5 \times 10^3, 10^2\right)$, we see that the MSE of the standard estimator is clearly lower than that of the variance deconvolution estimator for $\mathbb{S}_1$ and $\mathbb{S}_5$. Both of these indices are very close to zero (see Figure 12); in this case, the higher variance of the variance deconvolution estimator outweighs the bias of the standard estimator. In the second combination, we have increased N_ξ by a factor of 10 and decreased N_η by the same factor to keep C constant. The variance deconvolution estimator benefits from this configuration, with a MSE that is lower than that of the standard estimator at most locations in x.

This pattern is consistent across QoIs: when indices are close to zero the variance of the variance deconvolution

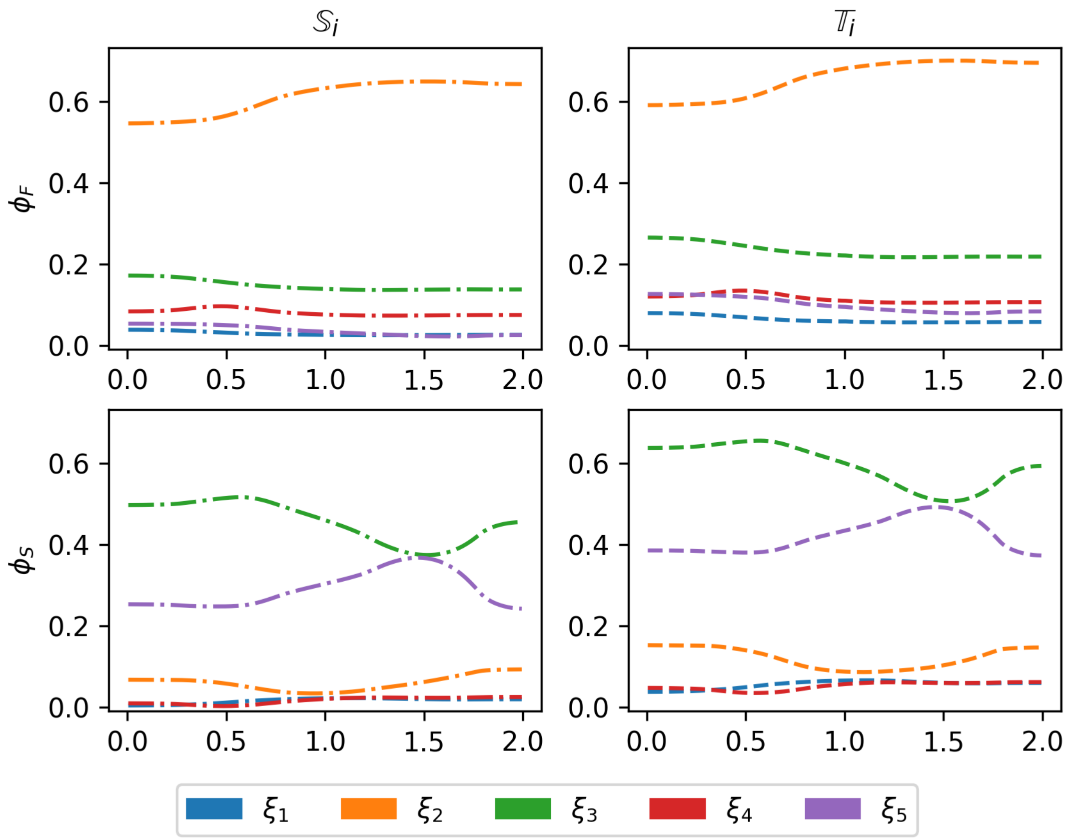

Figure 12: Full set of first- and total- order indices of ϕ_F and ϕ_S using $N_\xi = 5 \times 10^5$, $N_\eta = 10^5$. Standard and corrected estimators exactly overlap. Uncertain factors: the densities of 1) the fuel, 2) the moderator, 3) and the control rod were allowed to vary uniformly ±70%; 4) the ratio of fuel-width to moderator-width and 5) the control-rod thickness were both allowed to vary uniformly between 0.2 and 0.8.

estimator can outweigh the bias of the standard estimator, and for a constant C the variance deconvolution estimator generally benefits from increasing the N_ξ at the expense of decreasing N_η. In Figure 14, we see this for $\mathbb{S}_i\,[\phi_S]$. For estimating $\mathbb{T}_i$, the correction in both the numerator and denominator makes the difference between the standard and variance deconvolution estimators more drastic. In Figures 15 and 16, we see that the variance deconvolution estimator outperforms the standard across x for both ϕ_F and ϕ_S.

We have shown, in this example and the analytic test case, that when increasing computational cost for more accurate estimates of $\mathbb{S}_i$ and $\mathbb{T}_i$, putting those computational resources towards increasing N_ξ with the variance deconvolution estimator will improve the accuracy of indices that are not near zero.

7. Conclusion

In this paper, we extend the variance deconvolution framework introduced in [26] for UQ to global sensitivity analysis (GSA). Sobol' indices are well-suited and widely used for GSA, and there has been abundant work over the past few decades on the most efficient sampling schemes and estimators for SIs. In this work, we analyze the effect on SIs when the underlying solver is stochastic, i.e., has some underlying inherent variability (e.g., Monte Carlo radiation transport solvers). We build on a previously-developed variance deconvolution estimator which, rather than computing parametric variance by over-resolving the stochastic solver, explicitly quantifies and removes the solver variance from the total observed variance. We show in closed-form that in general, a stochastic solver will introduce a bias to

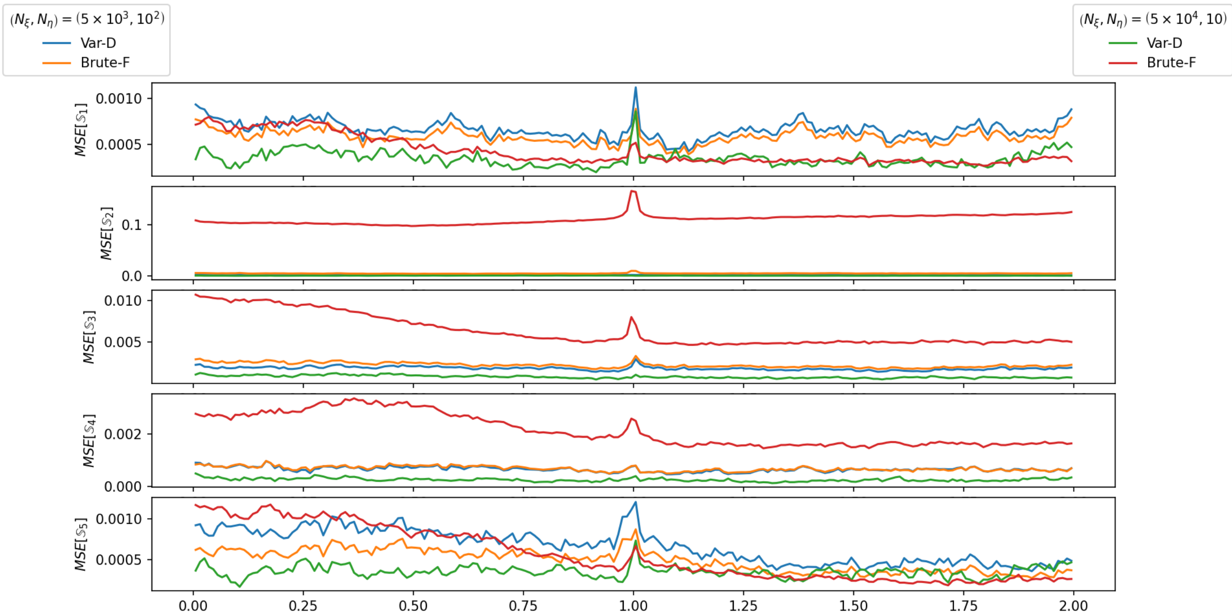

Figure 13: $MSE\left[\mathbb{S}_i\right]$ for ϕ_F, constant computational cost $C = \left(N_\xi \times N_\eta\right) = 5 \times 10^5$.

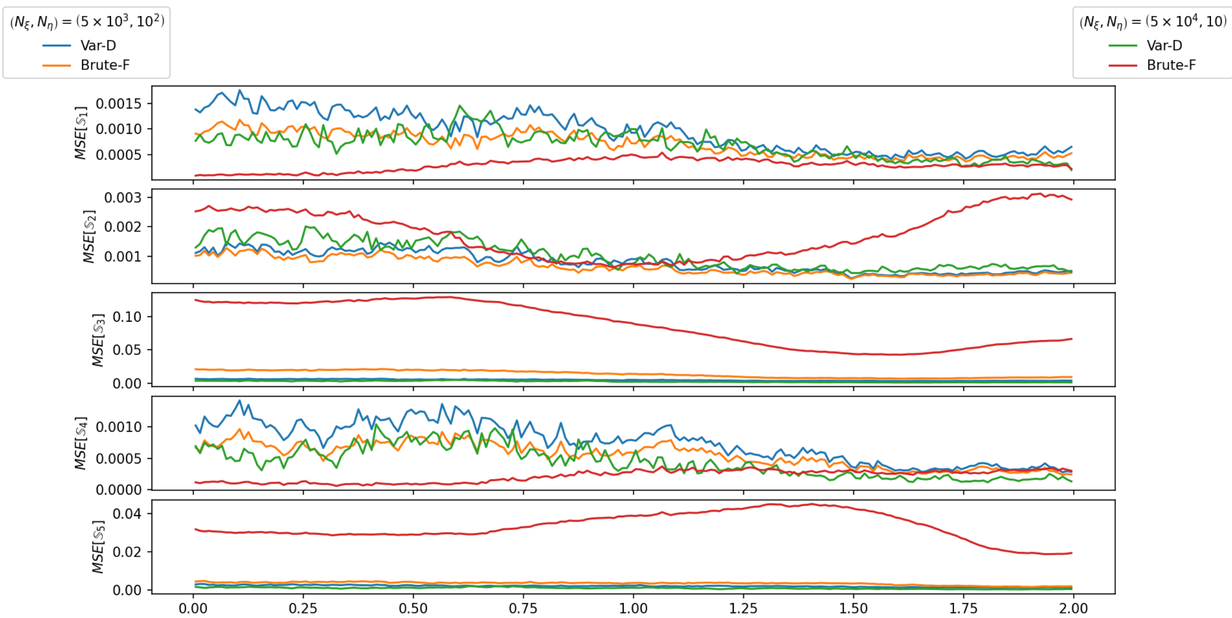

Figure 14: $MSE\left[\mathbb{S}_i\right]$ for ϕ_S, constant computational cost $C = \left(N_\xi \times N_\eta\right) = 5 \times 10^5$.

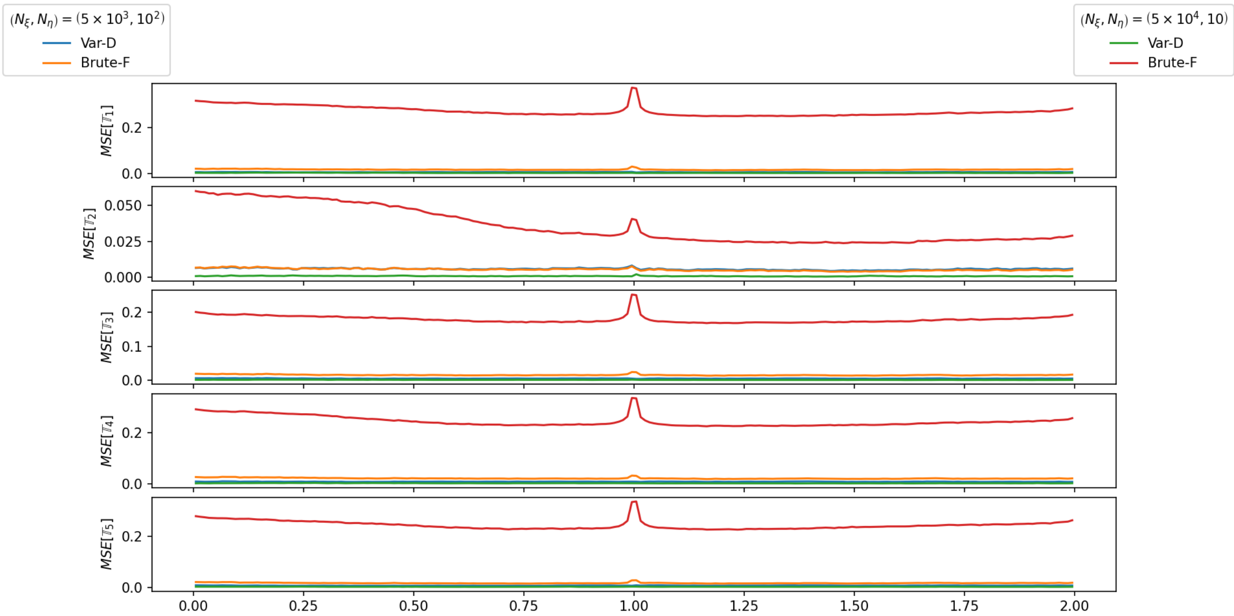

Figure 15: $MSE\,[\mathbb{T}_i]$ for ϕ_F, constant computational cost $C = (N_\xi \times N_\eta) = 5 \times 10^5$.

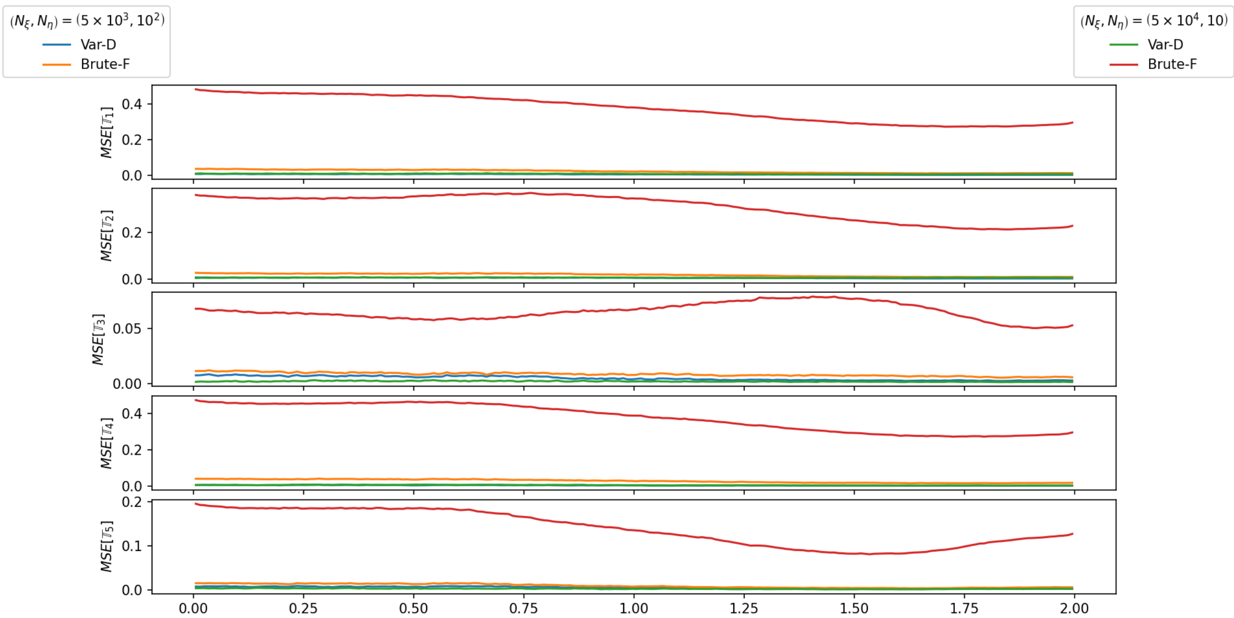

Figure 16: $MSE\,[\mathbb{T}_i]$ for ϕ_S, constant computational cost $C = (N_\xi \times N_\eta) = 5 \times 10^5$.

under-estimate the parametric first-order SIs and over-estimate the parametric total-order SIs. We find that though the variance deconvolution version of existing SI estimators can have a higher variance than its standard counterpart, the variance deconvolution version is able to accurately compute the indices for a reduced cost. When the solver noise contribution was approximately equal to the parameter noise, the variance deconvolution estimator saved 50X computational cost compared to the standard. When the solver noise was approximately double the parameter noise, the variance deconvolution estimator saved a 250X computational cost.

Appendix A. Mean-squared error from asymptotic normality

We set out to show the asymptotic normality of the estimators, from which their mean-squared errors follow. We assume that the estimators use a constant N_η stochastic solver samples per UQ realization.

The law of large numbers ensures that $\hat{\mathbb{S}}_i^{Va.}$ and $\hat{\mathbb{T}}_i^{Va.}$ converge to $\mathbb{S}_i$ and $\mathbb{T}_i$ almost surely, that is, $\lim_{N_\xi\to\infty} \hat{\mathbb{S}}_i^{Va.} = \mathbb{S}_i$ and $\lim_{N_\xi\to\infty} \hat{\mathbb{T}}_i^{Va.} = \mathbb{T}_i$.

The estimators $\hat{\mathbb{S}}_i^{St.}$ and $\hat{\mathbb{T}}_i^{St.}$ converge almost surely to $\mathbb{S}_{i,\tilde{Q}_{N_\eta}}$ and $\mathbb{T}_{i,\tilde{Q}_{N_\eta}}$ in the limit $N_\xi \to \infty$, and to $\mathbb{S}_i$ and $\mathbb{T}_i$ in the stricter limit $(N_\xi, N_\eta) \to \infty$.

Appendix A.1. First-order Estimators

In the following, we follow the steps of Janon et al. (2014) [51] and Azzini et al. (2021) [66] to establish that the asymptotic normality of $\hat{\mathbb{S}}_i^{Va.}$ is,

$$\lim_{N_\xi\to\infty} \sqrt{N_\xi}\left(\hat{\mathbb{S}}_i^{Va.} - \mathbb{S}_i\right) \sim \mathcal{N}\left(0, \mathbb{V}ar\left[\hat{\mathbb{S}}_i^{Va.}\right]\right), \tag{A.1}$$

with $\mathbb{V}ar\left[\hat{\mathbb{S}}_i^{Va.}\right]$ defined by Eq. (33), and that the asymptotic normality of $\hat{\mathbb{S}}_i^{St.}$ is,

$$\lim_{N_\xi\to\infty} \sqrt{N_\xi}\left(\hat{\mathbb{S}}_i^{St.} - \mathbb{S}_i \frac{N_\eta \mathbb{V}ar_\xi\left[Q\right]}{N_\eta \mathbb{V}ar_\xi\left[Q\right] + \mathbb{E}_\xi\left[\sigma_\eta^2\right]}\right) \sim \mathcal{N}\left(0, \mathbb{V}ar\left[\hat{\mathbb{S}}_i^{St.}\right]\right), \tag{A.2}$$

with $\mathbb{V}ar\left[\hat{\mathbb{S}}_i^{St.}\right]$ defined by Eq. (32).

Proof. We define a random vector X with mean μ_X, variance Σ_X, and sample mean $\overline{X}_{N_\xi} = {N_\xi}^{-1}\sum_{v=1}^{N_\xi} X_v$:

$$X = \begin{bmatrix} \tilde{Q}_{N_\eta}(\boldsymbol{B})\left[\tilde{Q}_{N_\eta}(\boldsymbol{A}_{\boldsymbol{B}}^{(i)}) - \tilde{Q}_{N_\eta}(\boldsymbol{A})\right] \\ \frac{1}{2}\left(\tilde{Q}_{N_\eta}(\boldsymbol{A}) - \tilde{Q}_{N_\eta}(\boldsymbol{B})\right)^2 \\ \frac{1}{2N_\eta}\left(\hat{\sigma}_\eta^2(A) + \hat{\sigma}_\eta^2(B)\right) \end{bmatrix} = \begin{bmatrix} \alpha \\ \beta \\ \gamma \end{bmatrix}, \tag{A.3}$$

$$\mu_X = \begin{bmatrix} \mathbb{V}ar_{\xi_i}\left[\mathbb{E}_{\xi_{\sim i}}\left[Q \mid \xi_i\right]\right] \\ \mathbb{V}ar\left[\tilde{Q}_{N_\eta}\right] \\ \mathbb{E}\left[\sigma_\eta^2\right]/N_\eta \end{bmatrix} = \begin{bmatrix} \mu_\alpha \\ \mu_\beta \\ \mu_\gamma \end{bmatrix}, \tag{A.4}$$

$$\Sigma_X = \begin{bmatrix} \mathbb{V}ar\left[\alpha\right] & \mathbb{C}ov\left[\alpha,\beta\right] & \mathbb{C}ov\left[\alpha,\gamma\right] \\ \mathbb{C}ov\left[\alpha,\beta\right] & \mathbb{V}ar\left[\beta\right] & \mathbb{C}ov\left[\beta,\gamma\right] \\ \mathbb{C}ov\left[\alpha,\gamma\right] & \mathbb{C}ov\left[\beta,\gamma\right] & \mathbb{V}ar\left[\gamma\right] \end{bmatrix}, \tag{A.5}$$

$$X_v = \begin{bmatrix} \tilde{Q}_{N_\eta}(\boldsymbol{B})_v\left[\tilde{Q}_{N_\eta}(\boldsymbol{A}_{\boldsymbol{B}}^{(i)})_v - \tilde{Q}_{N_\eta}(\boldsymbol{A})_v\right] \\ \frac{1}{2}\left(\tilde{Q}_{N_\eta}(\boldsymbol{A})_v - \tilde{Q}_{N_\eta}(\boldsymbol{B})_v\right)^2 \\ \frac{1}{2N_\eta}\left(\hat{\sigma}_\eta^2(A)_v + \hat{\sigma}_\eta^2(B)_v\right) \end{bmatrix} \overset{\text{i.i.d}}{\sim} F(X). \tag{A.6}$$

From the central limit theorem (CLT), we have $\sqrt{N_\xi}\left(\overline{X}_{N_\xi} - \mu_X\right) \xrightarrow{d} \mathcal{N}_k\left(0, \Sigma_X\right)$.

We define a function $g(a,b,c) = \frac{a}{b-c}$ such that

$$g\left(\mu_X\right) = \frac{\mathbb{V}ar_{\xi_i}\left[\mathbb{E}_{\xi_{\sim i}}\left[Q \mid \xi_i\right]\right]}{\mathbb{V}ar\left[\tilde{Q}_{N_\eta}\right] - \frac{1}{N_\eta}\mathbb{E}_\xi\left[\sigma_\eta^2\right]} = \mathbb{S}_i \tag{A.7}$$

and

$$g\left(\overline{X}_{N_\xi}\right) = \hat{\mathbb{S}}_i^{Va.}. \tag{A.8}$$

The so-called Delta method [67] establishes that the asymptotic normality of $g\left(\overline{X}_{N_\xi}\right)$ is

$$\sqrt{N_\xi}\left(g(\overline{X}_{N_\xi}) - g(\mu_X)\right) \xrightarrow{d} \mathcal{N}\left(0, \nabla_{\mu_X}\,\Sigma_X\,\nabla_{\mu_X}^T\right),$$

where $\nabla_{\mu_X} = \nabla g(\mu_X) \neq 0$. Therefore, we find that the estimator $\hat{\mathbb{S}}_i^{Va.}$ is unbiased regardless of stochastic solver sampling size N_η.

To find $\nabla_{\mu_X}\Sigma_X\nabla_{\mu_X}^T$, we first find that the gradient ∇g is

$$\nabla g(a,b,c) = \left[\frac{1}{b-c}, \frac{-a}{(b-c)^2}, \frac{a}{(b-c)^2}\right] \tag{A.9}$$

$$\rightarrow \nabla_{\mu_X} = \left[\frac{1}{\mathbb{V}ar_\xi\left[Q\right]}, \frac{-\mathbb{S}_i}{\mathbb{V}ar_\xi\left[Q\right]}, \frac{\mathbb{S}_i}{\mathbb{V}ar_\xi\left[Q\right]}\right]. \tag{A.10}$$

Therefore, we find that the variance of the estimator is,

$$\mathbb{V}ar\left[\hat{\mathbb{S}}_i^{Va.}\right] = \frac{\mathbb{V}ar\left[\alpha - \mathbb{S}_i\left(\beta - \gamma\right)\right]}{\mathbb{V}ar_\xi^2\left[Q\right]}. \tag{A.11}$$

Replacing α, β, and γ with their expressions from Eq. (A.3) leads to the result in Eq. 33.

Analysis of standard estimator $\hat{\mathbb{S}}_i^{St.}$ follows by using the same α and β to define a random vector Y,

$$Y = \begin{bmatrix} \tilde{Q}_{N_\eta}(\boldsymbol{B})\left[\tilde{Q}_{N_\eta}(\boldsymbol{A}_{\boldsymbol{B}}^{(\boldsymbol{i})}) - \tilde{Q}_{N_\eta}(\boldsymbol{A})\right] \\ \frac{1}{2}\left(\tilde{Q}_{N_\eta}(\boldsymbol{A}) - \tilde{Q}_{N_\eta}(\boldsymbol{B})\right)^2 \\ 0 \end{bmatrix} = \begin{bmatrix}\alpha \\ \beta \\ 0\end{bmatrix}.$$

This leads to $g(\mu_Y) = \mathbb{S}_{i,\tilde{Q}_{N_\eta}}$ and $g(\overline{Y}_{N_\xi}) = \hat{\mathbb{S}}_i^{St.}$. Again from the Delta method, the asymptotic normality of $g(\overline{Y}_{N_\xi})$ is

$$\sqrt{N_\xi}\left(g(\overline{Y}_{N_\xi}) - g(\mu_Y)\right) \xrightarrow{d} \mathcal{N}\left(0, \nabla_{\mu_Y}\,\Sigma_X\,\nabla_{\mu_Y}^T\right).$$

Therefore, we find that $\hat{\mathbb{S}}_i^{St.}$ is a biased estimator of $\mathbb{S}_i$,

$$\mathbb{B}ias^2\left[\hat{\mathbb{S}}_i^{St.}, \mathbb{S}_i\right] = \left(\mathbb{E}\left[\hat{\mathbb{S}}_i^{St.}\right] - \mathbb{S}_i\right)^2 \tag{A.12}$$

$$= \left(\mathbb{S}_{i,\tilde{Q}_{N_\eta}} - \mathbb{S}_i\right)^2 \tag{A.13}$$

$$= \mathbb{S}_i^2\left(\frac{\mathbb{V}ar_\xi\left[Q\right]}{\mathbb{V}ar\left[\tilde{Q}_{N_\eta}\right]} - 1\right)^2 \tag{A.14}$$

$$= \frac{\mathbb{S}_i^2}{{N_\eta}^2}\frac{\mathbb{E}_\xi^2\left[\sigma_\eta^2\right]}{\mathbb{V}ar^2\left[\tilde{Q}_{N_\eta}\right]}, \tag{A.15}$$

with variance

$$\mathbb{V}ar\left[\hat{\mathbb{S}}_i^{St.}\right] = \frac{\mathbb{V}ar\left[\alpha - \mathbb{S}_{i,\tilde{Q}_{N_\eta}}\beta\right]}{\mathbb{V}ar^2\left[\tilde{Q}_{N_\eta}\right]} \tag{A.16}$$

$$= \frac{1}{\mathbb{V}ar^2\left[\tilde{Q}_{N_\eta}\right]}\mathbb{V}ar\left[\alpha\right] + \frac{\mathbb{V}ar_\xi^2\left[Q\right]}{\mathbb{V}ar\left[\tilde{Q}_{N_\eta}\right]^4}\mathbb{S}_i^2\mathbb{V}ar\left[\beta\right] - 2\frac{\mathbb{V}ar_\xi\left[Q\right]}{\mathbb{V}ar\left[\tilde{Q}_{N_\eta}^3\right]}\mathbb{S}_i\mathbb{C}ov\left[\alpha,\beta\right]. \tag{A.17}$$

Replacing α and β with their definitions from Eq. (A.3) leads to the result in Eq. 32.

Appendix A.2. Total-order Estimators

In the same way, it can be established that the asymptotic normality of $\hat{\mathbb{T}}_i^{Va.}$ is

$$\lim_{N_\xi\to\infty}\sqrt{N_\xi}\left(\hat{\mathbb{T}}_i^{Va.} - \mathbb{T}_i\right) \sim \mathcal{N}\left(0, \mathbb{V}ar\left[\hat{\mathbb{T}}_i^{Va.}\right]\right), \tag{A.18}$$

with $\mathbb{V}ar\left[\hat{\mathbb{T}}_i^{Va.}\right]$ defined by Eq. (35), and that the asymptotic normality of $\hat{\mathbb{T}}_i^{St.}$ is,

$$\lim_{N_\xi\to\infty}\sqrt{N_\xi}\left(\hat{\mathbb{T}}_i^{St.} - \frac{\mathbb{T}_i N_\eta \mathbb{V}ar_\xi\left[Q\right] + \mathbb{E}_\xi\left[\sigma_\eta^2\right]}{N_\eta\mathbb{V}ar_\xi\left[Q\right] + \mathbb{E}_\xi\left[\sigma_\eta^2\right]}\right) \sim \mathcal{N}\left(0, \mathbb{V}ar\left[\hat{\mathbb{T}}_i^{St.}\right]\right), \tag{A.19}$$

with $\mathbb{V}ar\left[\hat{\mathbb{T}}_i^{St.}\right]$ defined by Eq. (34).

Proof. We define random vector X with mean μ_X, variance Σ_X, and sample mean $\overline{X}_{N_\xi} = {N_\xi}^{-1}\sum_{\nu=1}^{N_\xi} X_\nu$:

$$X = \begin{bmatrix} \frac{1}{2}\left(\tilde{Q}_{N_\eta}(\boldsymbol{B_A^{(i)}}) - \tilde{Q}_{N_\eta}(\boldsymbol{B})\right)^2 \\ \frac{1}{2}\left(\tilde{Q}_{N_\eta}(\boldsymbol{A}) - \tilde{Q}_{N_\eta}(\boldsymbol{B})\right)^2 \\ \frac{1}{2N_\eta}\left(\hat{\sigma}_\eta^2(\boldsymbol{A}) + \hat{\sigma}_\eta^2(\boldsymbol{B})\right) \\ \frac{1}{2N_\eta}\left(\hat{\sigma}_\eta^2(\boldsymbol{B_A^i}) + \hat{\sigma}_\eta^2(\boldsymbol{B})\right) \end{bmatrix} = \begin{bmatrix}\alpha\\ \beta\\ \gamma\\ \delta\end{bmatrix}, \tag{A.20}$$

$$\mu_X = \begin{bmatrix} \mathbb{V}ar\left[\mathbb{E}\left[Q \mid \xi_i\right]\right] \\ \mathbb{V}ar\left[\tilde{Q}_{N_\eta}\right] \\ \mathbb{E}\left[\sigma_\eta^2\right]/N_\eta \\ \mathbb{E}\left[\sigma_\eta^2\right]/N_\eta \end{bmatrix} = \begin{bmatrix}\mu_\alpha\\ \mu_\beta\\ \mu_\gamma\\ \mu_\delta\end{bmatrix}, \tag{A.21}$$

$$\Sigma_X = \begin{bmatrix} \mathbb{V}ar\left[\alpha\right] & \mathbb{C}ov\left[\alpha,\beta\right] & \mathbb{C}ov\left[\alpha,\gamma\right] & \mathbb{C}ov\left[\alpha,\delta\right] \\ \mathbb{C}ov\left[\alpha,\beta\right] & \mathbb{V}ar\left[\beta\right] & \mathbb{C}ov\left[\beta,\gamma\right] & \mathbb{C}ov\left[\beta,\delta\right] \\ \mathbb{C}ov\left[\alpha,\gamma\right] & \mathbb{C}ov\left[\beta,\gamma\right] & \mathbb{V}ar\left[\gamma\right] & \mathbb{C}ov\left[\gamma,\delta\right] \\ \mathbb{C}ov\left[\alpha,\delta\right] & \mathbb{C}ov\left[\beta,\delta\right] & \mathbb{C}ov\left[\gamma,\delta\right] & \mathbb{V}ar\left[\delta\right] \end{bmatrix}. \tag{A.22}$$

We define a function $g(a,b,c,c) = \frac{a-d}{b-c}$ such that

$$g\left(\mu_X\right) = \frac{\mathbb{E}_{\xi_{\sim i}}\left[\mathbb{V}ar_{\xi_i}\left[Q \mid \xi_{\sim i}\right]\right]}{\mathbb{V}ar\left[\tilde{Q}_{N_\eta}\right] - \frac{1}{N_\eta}\mathbb{E}_\xi\left[\sigma_\eta^2\right]} = \mathbb{T}_i \tag{A.23}$$

and

$$g\left(\overline{X}_{N_\xi}\right) = \hat{\mathbb{T}}_i^{Va.}. \tag{A.24}$$

We find that the gradient ∇g is

$$\nabla g(a,b,c,d) = \left[\frac{1}{b-c}, \frac{-(a-d)}{(b-c)^2}, \frac{(a-d)}{(b-c)^2}, \frac{-1}{b-c}\right] \tag{A.25}$$

$$\rightarrow \nabla_{\mu_X} = \left[\frac{1}{\mathbb{V}ar_\xi\left[Q\right]}, \frac{-\mathbb{T}_i}{\mathbb{V}ar_\xi\left[Q\right]}, \frac{\mathbb{T}_i}{\mathbb{V}ar_\xi\left[Q\right]}, \frac{-1}{\mathbb{V}ar_\xi\left[Q\right]}\right]. \tag{A.26}$$

Therefore, from the Delta method, we find that $\hat{\mathbb{T}}_i^{Va.}$ is an unbiased estimator for $\mathbb{T}_i$ regardless of size N_η, with variance

$$\mathbb{V}ar\left[\hat{\mathbb{T}}_i^{Va.}\right] = \frac{\mathbb{V}ar\left[\alpha - \delta - \mathbb{T}_i\left(\beta - \gamma\right)\right]}{\mathbb{V}ar_\xi^2\left[Q\right]}. \tag{A.27}$$

Replacing α, β, γ, and δ with their definitions from Eq. (A.20) leads to the result in Eq. 35.

Analysis of the standard estimator $\hat{\mathbb{T}}_i^{St.}$ follows by defining random vector Y:

$$Y = \begin{bmatrix} \frac{1}{2}\left(\tilde{Q}_{N_\eta}(\boldsymbol{B}_{\boldsymbol{A}}^{(i)}) - \tilde{Q}_{N_\eta}(\boldsymbol{B})\right)^2 \\ \frac{1}{2}\left(\tilde{Q}_{N_\eta}(\boldsymbol{A}) - \tilde{Q}_{N_\eta}(\boldsymbol{B})\right)^2 \\ 0 \\ 0 \end{bmatrix} = \begin{bmatrix} \alpha \\ \beta \\ 0 \\ 0 \end{bmatrix},$$

such that $g(\mu_Y) = \mathbb{T}_{i,\tilde{Q}_{N_\eta}}$ and $g(\overline{Y}_{N_\xi}) = \hat{\mathbb{T}}_i^{St.}$. From the Delta method, we find that $\hat{\mathbb{T}}_i^{St.}$ is a biased estimator for $\mathbb{T}_i$,

$$\mathbb{B}ias^2\left[\hat{\mathbb{T}}_i^{St.}, \mathbb{T}_i\right] = \left(\mathbb{E}\left[\hat{\mathbb{T}}_i^{St.}\right] - \mathbb{T}_i\right)^2 \tag{A.28}$$

$$= \left(\mathbb{T}_{i,\tilde{Q}_{N_\eta}} - \mathbb{T}_i\right)^2 \tag{A.29}$$

$$= \mathbb{T}_i^2\left(\frac{\mathbb{V}ar_\xi\left[Q\right]\mathbb{E}_{\sim i,\tilde{Q}_{N_\eta}}}{\mathbb{V}ar\left[\tilde{Q}_{N_\eta}\right]\mathbb{E}_{\sim i}} - 1\right)^2 \tag{A.30}$$

$$= \frac{\mathbb{T}_i^2}{{N_\eta}^2}\frac{\mathbb{E}_\xi^2\left[\sigma_\eta^2\right]\mathbb{V}_{\sim i}^2}{\mathbb{V}ar^2\left[\tilde{Q}_{N_\eta}\right]\mathbb{E}_{\sim i}^2}, \tag{A.31}$$

with variance

$$\mathbb{V}ar\left[\hat{\mathbb{T}}_i^{St.}\right] = \frac{\mathbb{V}ar\left[\alpha - \mathbb{T}_{i,\tilde{Q}_{N_\eta}}\beta\right]}{\mathbb{V}ar^2\left[\tilde{Q}_{N_\eta}\right]} \tag{A.32}$$

$$= \frac{1}{\mathbb{V}ar^2\left[\tilde{Q}_{N_\eta}\right]}\mathbb{V}ar\left[\alpha\right] + \frac{\mathbb{V}ar_\xi^2\left[Q\right]\mathbb{E}_{\sim i,\tilde{Q}_{N_\eta}}^2}{\mathbb{V}ar\left[\tilde{Q}_{N_\eta}\right]^4\mathbb{E}_{\sim i}^2}\mathbb{T}_i^2\mathbb{V}ar\left[\beta\right] - 2\frac{\mathbb{V}ar_\xi\left[Q\right]\mathbb{E}_{\sim i,\tilde{Q}_{N_\eta}}}{\mathbb{V}ar\left[\tilde{Q}_{N_\eta}^3\right]\mathbb{E}_{\sim i}}\mathbb{T}_i\mathbb{C}ov\left[\alpha,\beta\right]. \tag{A.33}$$

Replacing α and β with their definitions from Eq. (A.20) leads to the result in Eq. 34.

References

[1] N. R. Council, Assessing the Reliability of Complex Models: Mathematical and Statistical Foundations of Verification, Validation, and Uncertainty Quantification, The National Academies Press, Washington, DC, 2012. doi:10.17226/13395. URL https://nap.nationalacademies.org/catalog/13395/assessing-the-reliability-of-complex-models-mathematical-and-statistic

[2] K. Dowding, Overview of asme v&v 20-2009 standard for verification and validation in computational fluid mechanics and heat transfer, Tech. rep., V&V, UQ, and Credibility Processes Department, Sandia National Laboratories (2016).

[3] J. Helton, Uncertainty and sensitivity analysis for models of complex systems, in: F. Graziani (Ed.), Computational Methods in Transport: Verification and Validation, Springer, Berlin, 2008, pp. 207–228.

[4] A. Saltelli, et al., Global Sensitivity Analysis: The Primer, John Wiley & Sons, United Kingdom, 2008.
[5] R. Ghanem, D. Higdon, H. Owhadi, Handbook of Uncertainty Quantification, Springer International Publishing, Switzerland, 2017. doi:10.1007/978-3-319-12385-1.
[6] A. Saltelli, I. Sobol', About the use of rank transformation in sensitivity analysis of model output, Reliability Engineering and System Safety 50 (1995) 225–239.
[7] M. Ionescu-Bujor, D. Cacuci, A comparative review of sensitivity and uncertainty analysis of large-scale systems-i: Deterministic methods, Nuclear Science and Engineering 147 (3) (2004) 189–203. doi:10.13182/NSE03-105CR.
[8] D. Cacuci, M. Ionescu-Bujor, A comparative review of sensitivity and uncertainty analysis of large-scale systems-ii: Statistical methods, Nuclear Science and Engineering 147 (3) (2004) 204–217. doi:10.13182/04-54CR.
[9] I. Sobol', Sensitivity estimates for nonlinear mathematical models, Mathematical Modeling and Computational Experiment 1 (4) (1993) 407–414.
[10] T. Homma, A. Saltelli, Importance measures in global sensitivity analysis of model output, Reliability Engineering System Safety 52 (1) (1996) 1–17.
[11] T. Crestaux, O. L. Maitre, J.-M. Martinez, Polynomial chaos expansion for sensitivity analysis, Reliability Engineering & System Safety 94 (7) (2009) 1161–1172.
[12] K. Kontolati, D. Loukrezis, D. Giovanis, L. Vandanapu, M. Shields, A survey of unsupervised learning methods for high-dimensional uncertainty quantification in black-box-type problems, Journal of Computational Physics 464 (2022).
[13] S. Kucherenko, D. Albrecht, A. Saltelli, Exploring multi-dimensional spaces: a comparison of latin hypercube and quasi Monte Carlo sampling techniques, arXiv - University of Cornall (USA) (2015).
URL http://arxiv.org/abs/1505.02350
[14] G. Archer, A. Saltelli, I. Sobol', Sensitivity measure, anova-like techniques and the use of bootstrap, Journal of Statistical Computation and Simulation 58 (1997) 99–120.
[15] A. Saltelli, Making best use of model evaluations to compute sensitivity indices, Computer Physics Communications 145 (2002) 280–297.
[16] A. Puy, W. Becker, S. L. Piano, A. Saltelli, A comprehensive comparison of total-order estimators for global sensitivity analysis, International Journal for Uncertainty Quantification 2 (2022) 1–18.
[17] J. Crussell, T. Kroeger, A. Brown, C. Phillips, Virtually the same: Comparing physical and virtual testbeds, in: 2019 International Conference on Computing, Networking and Communications (ICNC), IEEE, 2019.
[18] G. Geraci, L. Swiler, B. Debusschere, Multifidelity uq sampling for stochastic simulations, 16th U.S. National Congress on Computational Mechanics (2021).
[19] A. Lattanzi, S. Subramaniam, Modeling Approaches and Computational Methods for Particle-Laden Turbulent Flows, Academic Press, 2023, Ch. 10 - Stochastic models.
[20] G. K. R. Korn, E. Korn, Monte Carlo Methods and Models in Finance and Insurance, CRC Press, 2010.
[21] B. Tripathy, M. Parimala, G. Reddy, Data Analytics in Biomedical Engineering and Healthcare, Academic Press, 2020, Ch. 11 - Innovative classification, regression model for predicting various diseases.
[22] E. Lewis, W. Miller, Computational Methods of Neutron Transport, American Nuclear Society, La Grange, Illinois, 1993.
[23] R. Larsen, M. Marx, An Introduction to Mathematical Statistics and Its Applications, 5th Edition, Pearson Education, Boston: Prentice Hall, 2012.
[24] A. B. Owen, Monte carlo theory, methods and examples (2013).
[25] D. Rochman, W. Zwermann, S. C. van der Marck, A. J. Koning, H. Sjöstrand, P. Helgesson, B. Krzykacz-Hausmann, Efficient use of monte carlo: Uncertainty propagation, Nuclear Science and Engineering 177 (2014). doi:10.13182/NSE13-32.
[26] K. Clements, G. Geraci, A. Olson, T. Palmer, A variance deconvolution estimator for efficient uncertainty quantification in monte carlo radiation transport applications, Journal of Quantitative Spectroscopy and Radiative Transfer 319 (2024). doi:10.1016/jqsrt.2024.108958.
[27] T. Rainforth, R. Cornish, H. Yang, A. Warrington, F. Wood, On nesting monte carlo estimators, Proceedings of the 35th International Conference on Machine Learning 80 (2018) 4264–4273.
[28] X. Zhu, B. Sudret, Global sensitivity analysis for stochastic simulators based on generalized lambda surrogate models, Reliability Engineering and System Safety 214 (2021). doi:10.1016/j.ress.2021.107815.
[29] B. Iooss, M. Ribatet, Global sensitivity analysis of computer models with functional inputs, Reliability engineering and system safety 94 (2009) 1194–1204.
[30] S. Da Veiga, F. Wahl, F. Gamboa, Local polynomial estimation for sensitivity analysis on models with correlated inputs, Technometrics 51 (2009) 452–463.
[31] A. Koning, D. Rochman, Towards sustainable nuclear energy: Putting nuclear physics to work, Annals of Nuclear Energy (2008).
[32] A. Koning, D. Rochman, Modern nuclear data evaluation with the talys code system, Nuclear Data Sheets 113 (12) (2012) 2841–2934.
[33] J. Hart, A. Alexanderian, P. Gremaud, Efficient computation of sobol' indices for stochastic models, SIAM Journal on Scientific Computing 39 (4) (2017) A1514–A1530. doi:10.1137/16M106193X.
[34] M. Jimenez, O. Le Maitre, O. Knio, Nonintrusive polynomial chaos expansions for sensitivity analysis in stochastic differential equations, SIAM Journal on Uncertainty Quantification 5 (1) (2017). doi:10.1137/16M1061989.
[35] A. Marrel, B. Iooss, S. Da Veiga, M. Ribatet, Global sensitivity analysis of stochastic computer models with joint metamodels, Statist Comput 22 (2012) 833–847. doi:10.1007/s11222-011-9274-8.
[36] T. Browne, L. L. Gratiet, J. Lonchampt, E. Remy, Stochastic simulators based optimization by gaussian process metamodels – application to maintenance investments planning issues, International Journal of Quality and Reliability Engineering 32 (6) (2016) 2067–2080.
[37] S. Azzi, B. Sudret, J. Wiart, Sensitivity analysis for stochastic simulators using differential entropy, International Journal for Uncertainty Quantification (2020). doi:10.1615/Int.J.UncertaintyQuantification.2020031610.
[38] A. J. Olson, Calculation of parametric variance using variance deconvolution, in: Transactions of the American Nuclear Society, Vol. 120, 2019.
[39] G. Geraci, A. Olson, Impact of sampling strategies in the polynomial chaos surrogate construction for monte carlo transport applications,

Proceedings of the International Conference on Mathematics and Computational Methods Applied to Nuclear Science and Engineering (2021) 76–86.
[40] G. Geraci, K. Clements, A. Olson, A polynomial chaos approach for uncertainty quantification of monte carlo transport codes, in: Proceedings of the American Nuclear Society M&C 2023, 2023.
[41] S. Hora, R. Iman, A comparison of maximum/bounding and bayesian/monte carlo for fault tree uncertianty analysis (no. sand85-2839), Tech. rep., Sandia National Laboratories (1986).
[42] T. Ishigami, T. Homma, An importance quantification technique in uncertainty analysis for computer models, in: Proceedings of the ISUMA'90, First International Symposium on Uncertainty Modelling and Analysis, University of Maryland, 1990.
[43] R. Iman, S. Hora, A robust measure of uncertainty importance for use in fault tree system analysis, Risk Analysis 10 (3) (1990) 401–403.
[44] A. Saltelli, P. Annoni, I. Azzini, F. Campolongo, M. Ratto, S. Tarantola, Variance based sensitivity analysis of model output. design and estimator for the total sensitivity index, Computer Physics Communications 181 (2010) 259–270.
[45] S. L. Piano, F. Ferretti, A. Puy, D. Albrecht, A. Saltelli, Variance-based sensitivity analysis: The quest for better estimators and designs between explorativity and economy, Reliability Engineering and System Safety 206 (2021).
[46] I. Sobol', On the distribution of points in a cube and the approximate evaluation of integrals, USSR Computational Mathematics and Mathematical Physics 7 (4) (1967) 86–112. doi:10.1016/0041-5553(67)90144-9.
[47] I. Sobol', Uniformly distributed sequences with an additional uniform property, USSR Computational mathematics and mathematical physics 16 (5) (1976) 236–242. doi:10.1016/0041-5553(76)90154-3.
[48] M. McKay, R. Beckman, W. Conover, Comparison of three methods for selecting values of input variables in the analysis of output from a computer code, Technometrics 21 (2) (1979) 239–245. doi:10.1080/00401706.1979.10489755.
[49] A. Puy, S. L. Piano, A. Saltelli, S. Levin, Sensobol: An r package to compute variance-based sensitivity indices, Journal of Statistical Software 102 (2022).
[50] G. Glen, K. Isaacs, Estimating sobol' sensitivity indices using correlations, Environmental Modelling and Software 37 (2012) 157–166. doi:10.1016/j.envsoft.2012.03.014.
[51] A. Janon, T. Klein, A. Lagnoux, M. Nodet, C. Prieur, Asymptotic normality and efficiency of two sobol' index estimators, ESAIM: Probability and Statistics 18 (3) (2014) 342–364. doi:10.1051/ps/2013040.
[52] L. Lilburne, S. Tarantola, Sensitivity analysis of spatial models, International Journal of Geographic Informational Systems (2009).
[53] T. Mara, O. Joseph, Comparison of some efficient methods to evaluate the main effect of compute model factors, Journal of Statistical and Computational Simulations (2008).
[54] M. McKay, Evaluating prediction uncertainty (no. nureg/cr-6311), Tech. rep., Nuclear Regulatory Commission (1995).
[55] A. Owen, Better estimation of small sobol' sensitivity indices, ACM Transactions on modeling and computer simulation (TOMACS) (2013).
[56] E. Plischke, E. Borgonovo, C. Smith, Global sensitivity measures from given data, European Journal of Operational Research (2013).
[57] M. Ratto, A. Pagano, P. Young, State dependent parameter metamodelling and sensitivity analysis, Computational Physics Communications (2007).
[58] I. Sobol', S. Tarantola, D. Gatelli, S. Kucherenko, W. Mauntz, Estimating the approximation error when fixing unessential factors in global sensitivity analysis, Reliability Engineering and System Safety 97 (7) (2007) 957–960.
[59] M. Jansen, Analysis of variance designs for model output, Computer Physics Communications 117 (1-2) (1999) 35–43. doi:10.1016/s0010-4655(98)00154-4.
[60] I. Azzini, T. Mara, R. Rosati, Monte carlo estimators of first- and total-orders sobol' indices, this is on arXiv and the pdf says it's an Elsevier preprint. However, I can't find a published version. (2020). doi:10.48550/arXiv.2006.08232.
[61] I. Sobol', Global sensitivity indices for nonlinear mathematical models and their monte carlo estimates, Mathematics and Computers in Simulation 55 (1-3) (2001) 271–280. doi:10.1016/s0378-4754(00)00270-6.
[62] H. Monod, C. Naud, D. Makowski, Uncertainty and Sensitivity Analysis for Crop Models, 1st Edition, Elsevier Science, 2006, pp. 35–100, eBook ISBN: 9780080461939.
[63] S. Razavi, H. Gupta, A new framework for comprehensive, robust, and efficient global sensitivity analysis: 1. theory, Water Resources Research 52 (1) (2016) 423–439. doi:10.1002/2015wr017559.
[64] S. Razavi, H. Gupta, A new framework for comprehensive, robust, and efficient global sensitivity analysis: 2. application, Water Resources Research 52 (1) (2016) 440–455. doi:10.1002/2015wr017558.
[65] A. Saltelli, M. Ratto, S. Tarantola, F. Campolongo, Update 1 of: sensitivity analysis for chemical models, Journal of Chemistry 112 (5) (2012) PR1–PR21.
[66] I. Azzini, T. Mara, R. Rosati, Comparison of two sets of monte carlo estimators of sobol' indices, Environmental Modelling and Software 144 (2021) 105167. doi:10.1016/j.envsoft.2021.105167.
[67] A. Van der Vaart, Asymptotic Statistics, Cambridge University Press, 2000.
[68] I. Lux, L. Koblinger, Monte Carlo Particle Transport Methods: Neutron and Photon Calculations, CRC Press, 1991.
[69] N. S. Committee, Benchmark on deterministic transport calculations without spatial homogenization, Tech. rep., Organization for Economic Co-operation and Development Nuclear Energy Agency (OECD/NEA) (2005).